Fabrication of Random Hole Optical Fiber Preforms by Silica Sol-Gel Processing

Frederick Paa Kwesi Ellis

Thesis to be submitted to the Faculty of the Virginia Polytechnic Institute and State University in partial fulfillment of the requirements for the degree of

Master of Science
In
Materials Science and Engineering

Gary Pickrell, Co-Chair
Anbo Wang, Co-Chair
Alex Aning

February 19th, 2004
Blacksburg, Virginia

Keywords: Sol-Gel, Holey Fiber, Photonic Band Gap, Critical Point Drying

Fabrication of Random Holed Optical Fiber Preforms by Silica Sol-Gel Processing

Frederick Paa Kwesi Ellis

(ABSTRACT)

Conventional fibers are comprised of a solid glass core and solid glass cladding often protected by a thin polymer sheath. The finely tuned difference in refractive indices, for step index-fibers, is achieved by doping the core with germanium or elements with similar effects. Holey fibers (including photonic crystal fibers) comprise of a pure silica core, and a pure but porous silica cladding of air holes [1]. This provides a huge difference in the refractive indices on the cladding and core without doping. This translates into radiation resistant fibers with very low losses and very robust to high temperatures to mention a few [2]. Several successful attempts have been made for ordered holey optical fibers since the initial publication by Knight et al; random holey optical fibers, which can be just as effective, have yet to be fabricated [3].

Sol-gel processing of silicon alkoxides can be used to fabricate silica monoliths of tailored pore densities and sizes [4]; this makes the process attractive for random holey fiber preform manufacturing. Similar attempts have been made by Okazaki et al [5] to make conventional optical fibers. This paper chronicles efforts to make random holey fiber optical preforms from silica sol-gel monoliths, characterized for some structural properties. Silica monoliths can be made by hydrolysis and condensation of TEOS (tetraethylorthosilicate) or TMOS (tetramethylorthosilicate). These can be catalyzed in a single step or two-step process, aged and dried at ambient pressures and temperatures, as well as by supercritical fluid extraction of CO_2. Mechanical strengthening techniques as described by Okazaki [5] have also been employed. The silica gel monoliths are characterized by helium pycnometry and scanning electron microscopy. Various shapes and densities of silica monoliths have been prepared and characterized. Some of these have also drawn into fibers to demonstrate their viability.

Acknowledgements

I would like to thank my co-chairs and advisors Dr. Gary Pickrell and Dr. Anbo Wang for giving me an opportunity to work them. My appreciation is also extended to all the members of the Center for Photonic Technology for their invaluable support and encouragement. I would like to thank my committee member, Dr. Alex Aning for convincing me to pursue an advanced degree in Materials Science and Engineering and Dr. Clark and Dr. Reynolds for their efforts to ensure that I stayed in the department.

Scott Reed of Sandia National Labs provided unparalleled technical expertise and insight into sol gel processing. My gratitude also goes out to Carlos Folgar and Ashley White both of the MSE department with whom I had extensive discussions on the subject matter. I would like to acknowledge the invaluable assistance of Stephen McCartney, SEM Spectroscopist for his assistance and expert knowledge.

Additionally, I would also like to thank all the excellent Professors at Virginia Tech who shared their wealth of knowledge with me through various means. I'd also like to thank my friends -- both near and far who had to endure my occasional complaints when my research wasn't going as planned. Thanks for being there to keep me honest -- you know yourselves.

Finally, I would like to thank my family again for always praying for me, and believing that God’s mercy and grace would help me make it through this endeavor.

Table of Contents

Table of Figures

Table of Equations

Chapter 1 Introduction and Literature Review

1.1 Photonic Band Gap Materials

1.1.1 Introduction

Lord Rayleigh was the first to study the propagation of electromagnetic waves in the late nineteenth century [2]. Photonic band gap (PBG) materials were 'discovered' in the early 1990s as documented by two independent publications by Eli Yoblanovich and Sajeev John at the end of the previous decade [2]. The photonic band gap is a range of frequencies in which light cannot travel through a structure [2]; materials which express this characteristic are referred to as photonic band gap materials. Rayleigh was actually studying one-dimensional photonic band gap materials (a.k.a. photonic crystals) but concepts developed by Yoblanovich and John led to the realization of two-dimensional and eventually three-dimensional photonic crystals [2].

K. M. Ho et al [6] define photonic band gap crystals as periodic dielectric structures which possess a frequency gap in which electromagnetic waves are forbidden. This is somewhat analogous to electronic band gaps which are bands of energy within which electrons cannot occupy. It is obvious that such characteristics of a material will be critical for the fabrication of index guided holey optical fibers as their function is to guide signals without losing it in the cladding.

1.1.2 Literature Review

Three types of photonic band gap materials have been identified, one-, two-, and three-dimensional materials by virtue of their versatility and ability to restrict the propagation of electromagnetic waves. One-dimensional photonic band gap materials are dielectrics periodic in only one direction, its structure is comprised of periodically alternating materials of distinct dielectric constants [7]. Their structure enables them to prevent the propagation of electromagnetic waves within certain frequency ranges. Strategic introduction of defects in the structure increases the functionality of one-dimensional photonic crystals. It enables them to confine specific light modes within their structure and reflect electromagnetic waves at practically normal angles of incidence [7]. As such, filters and dielectric mirrors are the most common applications of such crystals. Another application is the fabrication one-dimensional Bragg fibers.

Two-dimensional photonic crystals are periodic along two axes and homogeneous in the third axis. One such structure can be a lattice of periodically arranged dielectric cylinders akin to a two-dimensional arrangement of quarters, stacked in the third dimension. With this arrangement periodicity is only present in the axial plane [8]. The converse of the above arrangement, i.e., a long piece of dielectric material hole periodically drilled along its long axis also serves as a two-dimensional photonic band gap material. Incident electromagnetic waves at any angle, within the two-dimensional plane, will experience a complete band gap. If, however, the incident waves are not in the two-dimensional plane they will not encounter the set periodicity of the lattice and this will result in a decrease in the band gap characteristics of the photonic crystal [8].

Three-dimensional photonic materials provide the best controls of photons. The most studied structures are based on the diamond lattice structure. One form has dielectric spheres at the lattice points while another, yoblanovite, is derived from a block of dielectric material with spherical holes at the lattice points connected by cylindrical columns [2]. For materials with high dielectric constants, complete band gaps have been theories have been proposed [9] and verified experimentally.

A summary of all the different dimensions of photonic band gap materials reveals the following:

One-dimensional materials exhibit the photonic band gap effect only on electromagnetic waves which are normally incident on its surface or at least close to the normal

Two-dimensional materials are limited only by the plane in which the angles of incident originate while three-dimensional materials are limited primarily by their methods of fabrication. This makes two-dimensional photonic band gap materials the materials of choice for the fabrication of holey optical fibers.

1.2 Holey Fibers

1.2.1 Introduction

The principal motivation of this research project was to develop a technique to fabricate optical fiber preforms of controlled porosity in controlled spatial locations. Random-holed optical fibers are one of two primary types of holey fibers; the other type is ordered-holed holey fibers. Holey fibers differ from conventional fibers by having a series of holes running through the cladding region of the fiber versus

the dense cladding of the latter. Conventional fibers are capable of confining light in the cores of the fibers by having been specifically doped with atoms (e.g. germanium) or heavier molecules which increase the refractive index beyond that of pure silica (n ~ 1.45) cladding regions. Conversely, the cladding could be doped with lighter molecules to reduce its refractive index.

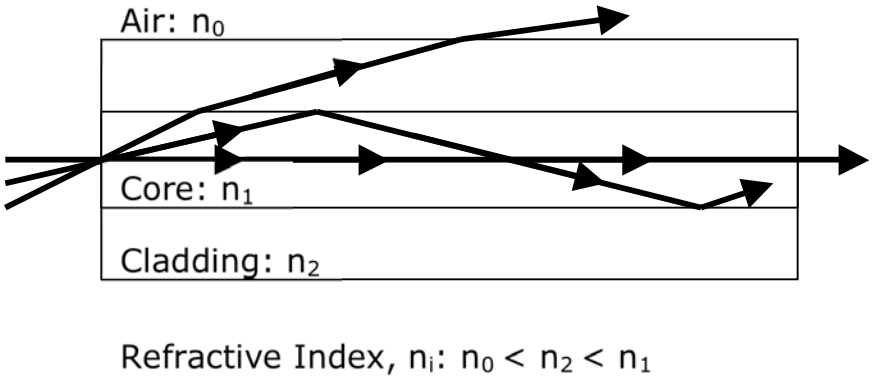

Figure 1.2.1: Signal Transmission in Index Guided Fibers

Holey fibers on the other hand, produce the refractive index difference by the presence of holes (n ~1.00) in the cladding region which lowers the average refractive index of the cladding region. The a lower average refractive index in the cladding of the optical fiber ensures that light traveling in the denser core remains confined. The primary methods by which light is guided through the core of the fibers is either two dimensional photonic bandgap effects (for low index guiding fibers) or by average/step index effects (for high index guiding fibers).

Until recent work by Monro et al [10] only ordered-holed optical fibers were thought to be suitable for adequate confinement of electromagnetic signals. Monro et al provided direct confirmation of the volume averaging effects. They accomplished this feat by numerical modeling which even accounted for complex asymmetric structures and modes accurately. Their results suggested that randomly distributed holes can be just as effective as in ordered holes in holey fibers.

1.2.2 Literature Review

The first mention of holey fibers (a.k.a. photonic crystal or microstructured fibers) was by British researchers J.C. Knight et al [11] as early as 1996. Their purpose for inventing photonic crystals fibers

was to fill the void for materials capable of periodically modulating refractive indices on the order of optical wavelengths in a fiber. Their fibers had unique hexagonal cross section and an ordered arrangement of holes in the cladding region. As previously noted, a few years later, Monro et al found it unnecessary for the holes to be ordered for hence coining the name holey fibers to put both ordered and random holed optical fibers under one umbrella [10].

As their names suggest, ordered-holed optical fibers have a definite, usually geometric, arrangement of holes in the cladding; random-holed optical fibers on the other hand have randomly distributed holes in their cladding. Random-holed optical fibers have been made by the careful processing of gas producing powders (GPP) and pure silica powders in a draw tower [12]. Figure 1.2.2 below is an SEM micrograph of such a fiber.

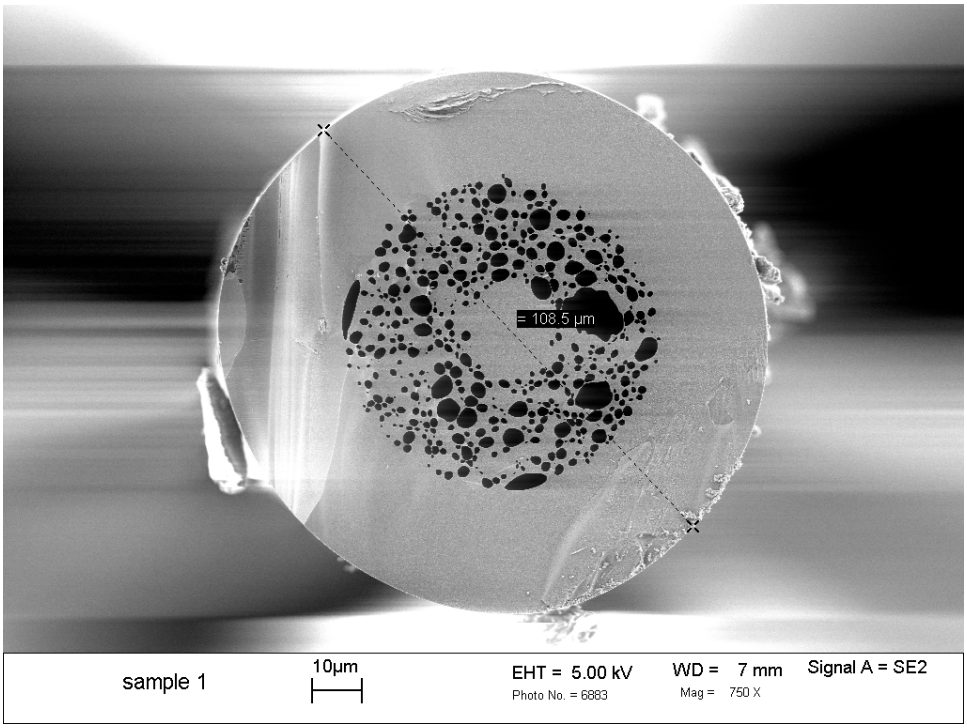

Figure 1.2.2: Random Hole Optical Fiber Fabricated by the GPP Method

In summary, their fibers are made by drawing the preform assembly which comprises of a dense fused silica core surrounded by a porous cladding region which is protected by a fused silica a tube, shown below in figure 1.2.3.

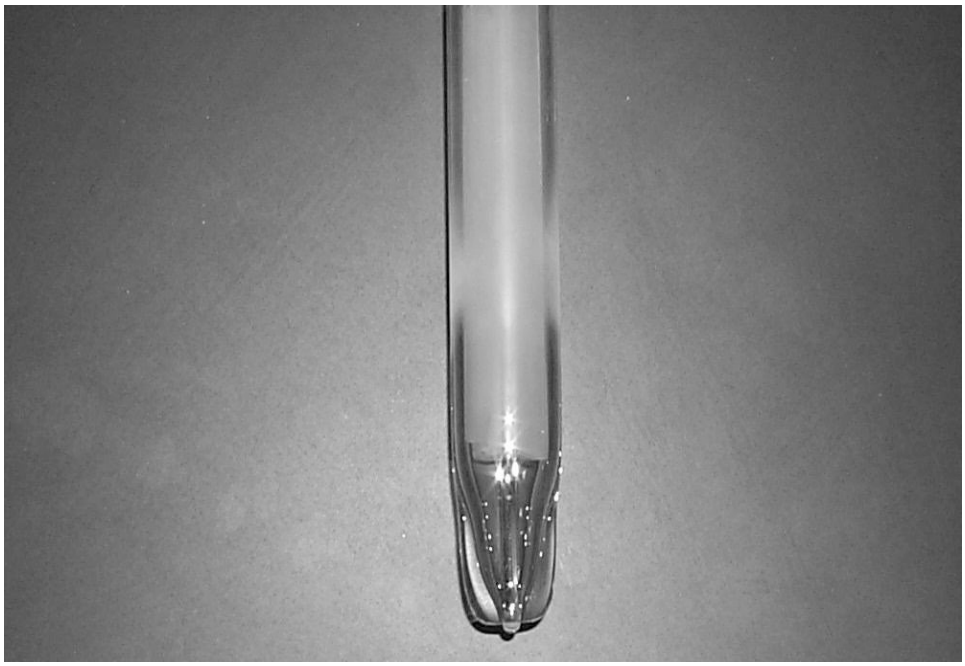

Figure 1.2.3: Preform assembly [12]

During the drawing process the spherical pores in the cladding manufactured via sol gel processing will be drawn out into long cylindrical pores running along the length of the fiber. This is depicted by Pickrell et al [12] in the micrograph shown below.

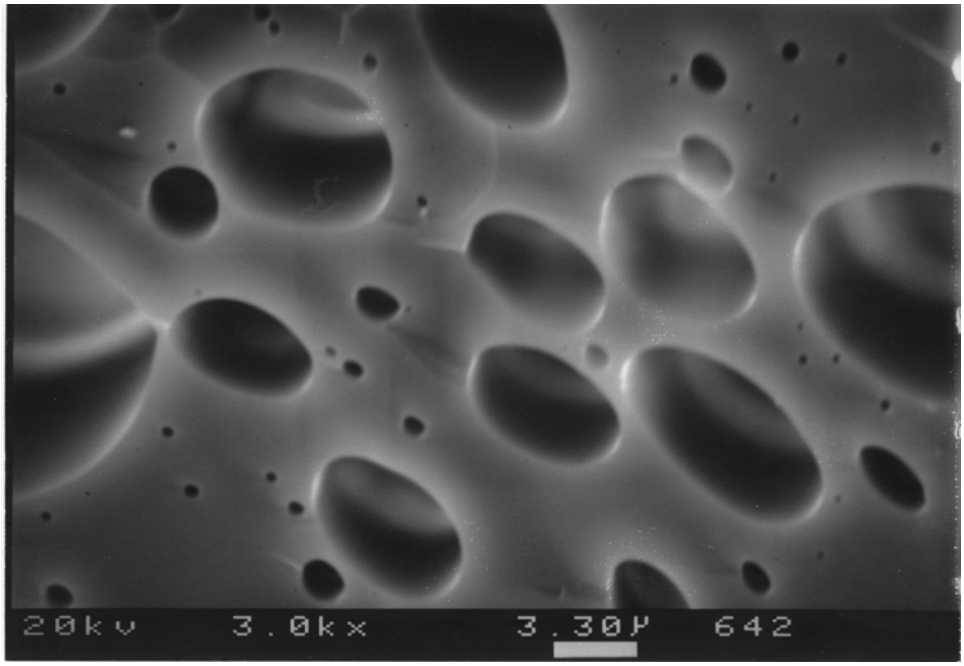

Figure 1.2.4: Representative fracture cross section of hand-drawn fiber [12]

Preliminary tests on fiber drawing can be achieved inexpensively by subjecting the gel monoliths to transition temperatures and drawing them.

Preliminary trails implementing aerogels as choice materials for the cladding region has shown significant promise. The figure below is the SEM micrograph of a fiber produced using a high porosity (97%) aerogel. The porosity of the cladding was so high that aerogel cladding withered away during the fiber drawing procedure; it has been suggested that higher density aerogels would yield more favorable results [12].

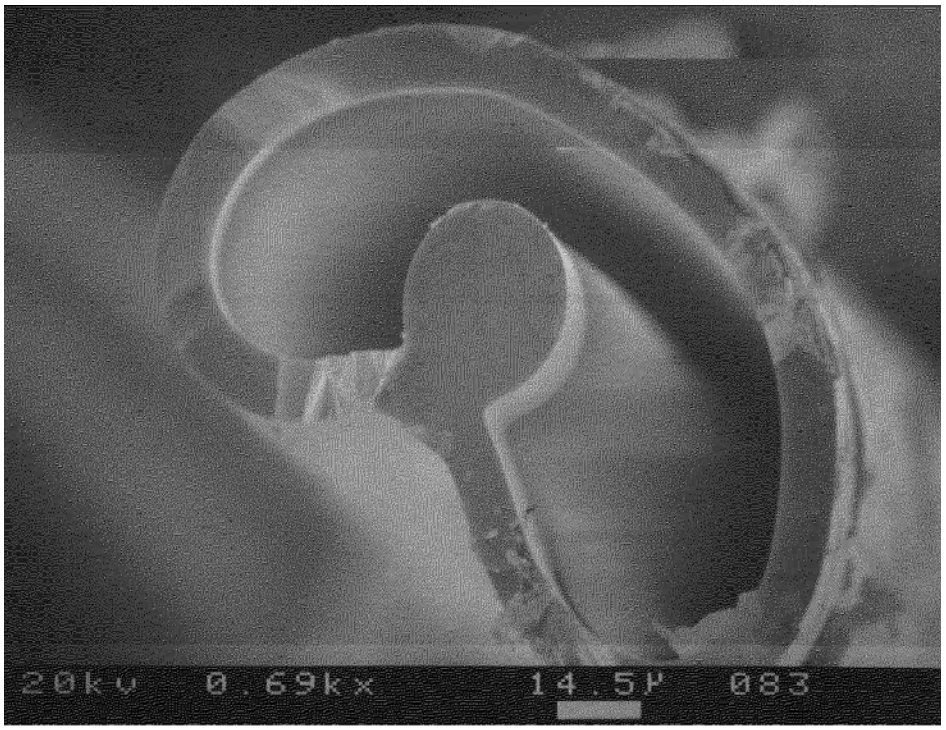

Figure 1.2.5: SEM of random holey optical fiber with sol gel derived cladding material [12]

Several advantages of using aerogels versus the above mentioned method include its higher levels of homogeneity (of both pore size and material composition), stronger confinement, versatility to incorporate future modifications for attenuation of fibers, and, lower processing costs.

Various methods of fabrication of holey fibers have addressed specific properties that compare to or exceed those of conventional fibers. The most deficient performance of holey fibers is the loss of signal

measured in dB/km. Compared to standard conventional fibers with losses of 0.2 dB/km, the best reported value for holey fibers is 0.58 dB/km at wavelengths of 1.55 μms by Blaze Photonics, a company based in the United Kingdom [4]. A majority of their losses were attributed to fiber geometry, Rayleigh scattering and hydroxyl absorption. In most other areas, holey fibers have exceedingly outperformed conventional fibers. Endlessly Single-Mode Fibers (ESMF) have been reported by Birks et al [13] to remain in single-mode for all wavelengths. Other important properties of endlessly single-mode fibers include their extreme nonlinearity and their anomalous dispersions of visible electromagnetic spectrum.

Although sol-gel processing is an old technique, this is the first attempt utilizing it to fabricate random holed optical fibers.

1.3 Sol Gel Processing

1.3.1 Introduction

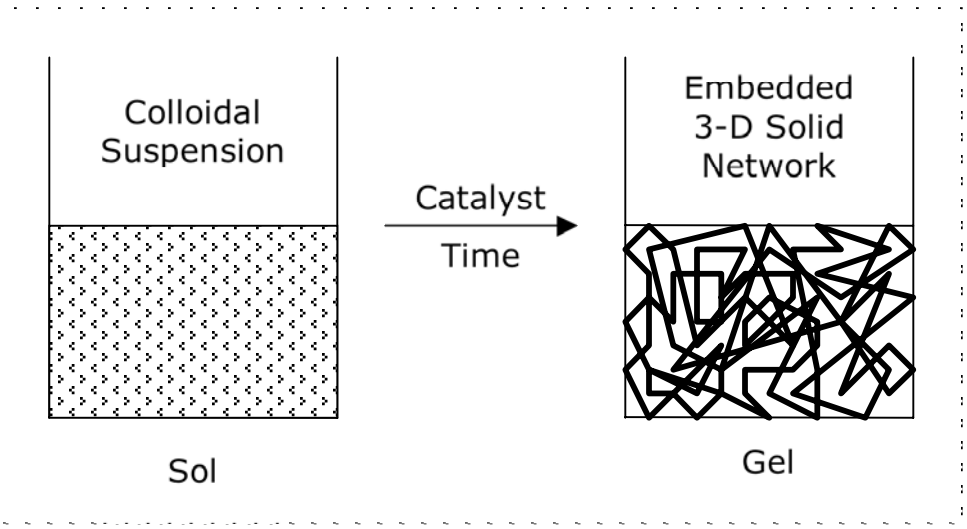

Figure 1.3.1 Sol-Gel Process

Sol-gel processing involves the formation of colloidal suspension of solid particles in a liquid– known as the sol, and the subsequent formation of a 3-dimensional solid network in a continuous liquids phase – known as the gel. The earliest documentation of sol-gel processing is credited to a French Engineer, Jacques-Joseph Ebelmen. He found that the metal alkoxide resulting from the alcolysis of Silicon (IV) Chloride gels upon exposure to the atmosphere during the earlier half of the 19th century [15]. Precursors, catalysts, and, conditions

under which sol-gel processing is carried directly dictates the processing times, structures, properties, characteristics and consequently the applications of the gels produced.

However, fueled by the curiosity of the gel structure by the scientific community and his personal interest in supercritical fluids, Samuel Kistler made a breakthrough on the morphology of the gel structure. About eight decades ago scientists postulated that gels were essentially composed of solid and liquid phases which were independent of each other, but had no means of proving this hypothesis. To prove this, they needed to invent a way to separate the phases without destroying either of them. So in 1932, applying his extensive knowledge of supercritical fluids, Kistler devised a method of extracting the liquid in its supercritical form thus leaving the solid skeleton of the gel that we call the aerogel without destroying it [16]. Today this is referred to as supercritical extraction (SCE) or critical point drying (CPD).

1.3.2 Literature Review

The sol-gel process involves the formation of a colloidal suspension (sol) and gelation of the sol to form a network in a continuous liquid phase (gel). Our desired product is a network of silicon dioxide molecules with a tetragonal structure akin to that of diamond. As such our precursors for the reactions should include sources for silicon and oxygen; of these the most reliable are tetraalkoxysilanes [14]. Tetramethylorthosilicate (TMOS) and tetraethylorthosilicate (TEOS) are the most frequently used. These silicates are hydrolyzed by acid or base catalyzed reactions to form monomers in a colloidal suspension (i.e., sols) which polymerize, by condensation, to form gels. Sol-gel processing is often characterized by the phenomena that dominate the various sections of its timeline. A typical series of characterization would include hydrolysis, polycondensation i.e., polymerization by condensation, gelation, washing and aging – physical processes to strengthen gel structure, then drying and if necessary densification.

1.3.2.1 Hydrolysis and Condensation

Three types of reversible reactions are generally used to describe the sol-gel processing of silicon alkoxides, they are: hydrolysis, water condensation and alcohol condensation.

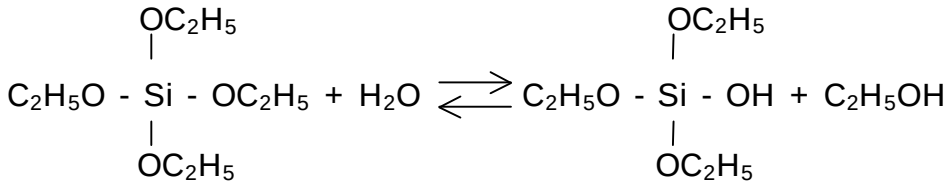

Equation 1.3.2.1: Acid-/Base-catalyzed Hydrolysis/esterification of a tetraalkoxysilane

Hydrolysis can either be acid catalyzed or base catalyzed to yield the same results – chemically speaking. Depending on the catalyst however, the mechanism for catalysis varies substantially and dictates the microstructure of the gels.

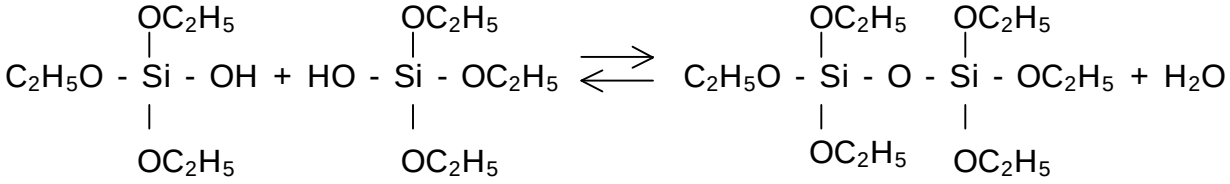

Equation 1.3.2.2: Water Condensation/Hydrolysis of a silanols

Water condensation is so called because it concludes with the formation of one molecule of water; it also occurs between two molecules of silanols as Equation 1.3.2.2 shows. Alcohol condensation differs from the former by tetraalkoxysilane and a silanol to form an alcohol as the by-product. See equation 1.3.2.3 below.

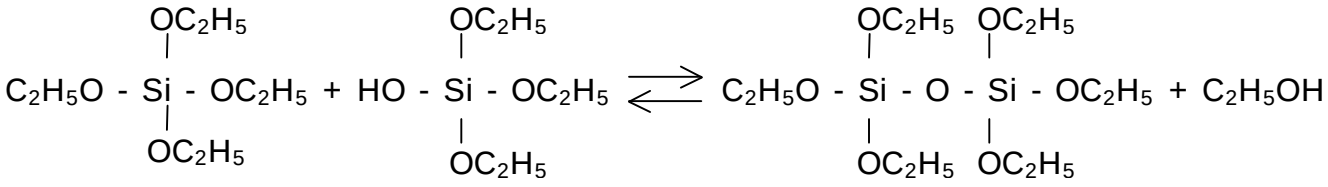

Equation 1.3.2.3: Alcohol Condensation/Alcoholysis between a silane and a silanol group

One problem encountered when trying to perform these reactions is the fact that alkoxides and water are immiscible, to resolve this, a homogenizing agent, an alcohol is implemented. For instance, when TEOS is the precursor, ethanol is the alcohol of choice since it is already a by-product of the process; likewise if TMOS is used, methanol is the most suitable homogenizing agent. Sol-Gel processing

reactions are catalyzed by acids, bases or both. The consequences of the catalyst used are eventually manifested in the microstructure of the resulting gel.

1.3.2.2 Gelation

As condensation progresses the reaction mixture is first converted to the sol. The sol is defined as a colloidal suspension of solid particles in a liquid. The solid particles represent the initial products of the condensation reactions. With the commencement of polycondensation, these dimers form even larger polymers as described by the process of percolation theory. This continues until a giant macromolecule of silica has been formed which spans through the entire solution -- this is the gel. As the polymer increases in size, its density decreases because the volume increases at an even faster rate. The classical theory, in conjunction with kinetic models and experimental studies, and the aforementioned percolation theory have been used to complement each other in describing the gelation process. Gelation usually occurs at the reaction temperatures unless otherwise stated.

1.3.2.3 Aging

It is during this phase that changes in structure and hence properties of the gels occur; aging allows physical processes to strengthen gel structure. The primary mechanism by which this occurs is Ostwald ripening. According to Brinker and Scherer [17], Ostwald ripening is facilitated by dissolution and re-precipitation of silica to regions of weaker structural integrity. Also, because polycondensation does not cease to occur, the smaller polymers, colloids or clusters condense into the larger molecules further strengthening the silica structure. An underlining driving force for aging is that it progresses with a decrease in surface energy and hence a corresponding decrease in total surface area. This probably explains why syneresis – the phenomenon of spontaneous shrinkage, has also been observed during aging. Syneresis is facilitated by the preferential affinity between clusters versus the pore liquid. In this study, aging was usually carried out at or just about the reaction temperature.

1.3.2.4 Drying

Drying is the most critical section of sol gel-processing. It proceeds with appreciable shrinkage of the gel structure; the volume changes

observed are usually on the order of the amount of pore liquid that evaporates [14]. As a matter of fact, the evaporation drives shrinkage: as the pore liquid evaporates from the surface of the gel, the solid gel network recedes, by capillary tension, towards the remaining pore liquid at a constant rate. This continues until the gel structure stiffens up and can no longer be held under the pore liquid by capillary forces. Capillary tension increases as the remaining pore liquid evaporates and diffuses out of the gel. This eventually causes the gel structure to fracture or crack.

Known ways of preventing or reducing the excessive capillary forces include the fabrication of large pore size gels and by replacing the pore liquid with another liquid of low surface tension. Larger pore sizes can be obtained by fabrication with base catalyzed reactions as previously noted. Application of drying control chemical additives (DCCA) also increases the pore sizes while simultaneously strengthening the gel structures. Aging is also encouraged as it strengthens the gel structure thus increasing the magnitudes of capillary forces which it can withstand [17]. As previously mentioned supercritical fluid extraction by critical point drying is also an effective means of avoiding cracking during the drying stages of sol-gel processing. In this study, several drying techniques were employed, from the use of DCCA, ambient temperature and pressure drying, through ambient pressure and temperature profile drying to critical point drying.

1.3.2.5 Densification

Densification is only necessary if further control of the density is required. Depending on the type of catalyst, which determines the pore size of the original gel, total densification occurs between about 600^{o}C – 1200^{o}C [18]. Acid-catalyzed gels usually have higher initial skeletal densities and densify at temperatures closer to 600^{o}C. The larger pore sizes in base-catalyzed reactions need higher temperatures to consolidate. At these temperatures, the densities of the gels abruptly change to approach that of fused silica. Results by Pope and Mackenzie suggest that there is relatively less significance in the changes observed in the percent porosities of the gels under similar conditions [17].

1.3.3 Factors Affecting Sol-Gel Processing

The remainder of this chapter is devoted to the factors affecting sol-gel processing. The following is a concise overview of the factors taken into account during the experimental stages of the project.

1.3.3.1 Effect of Precursors

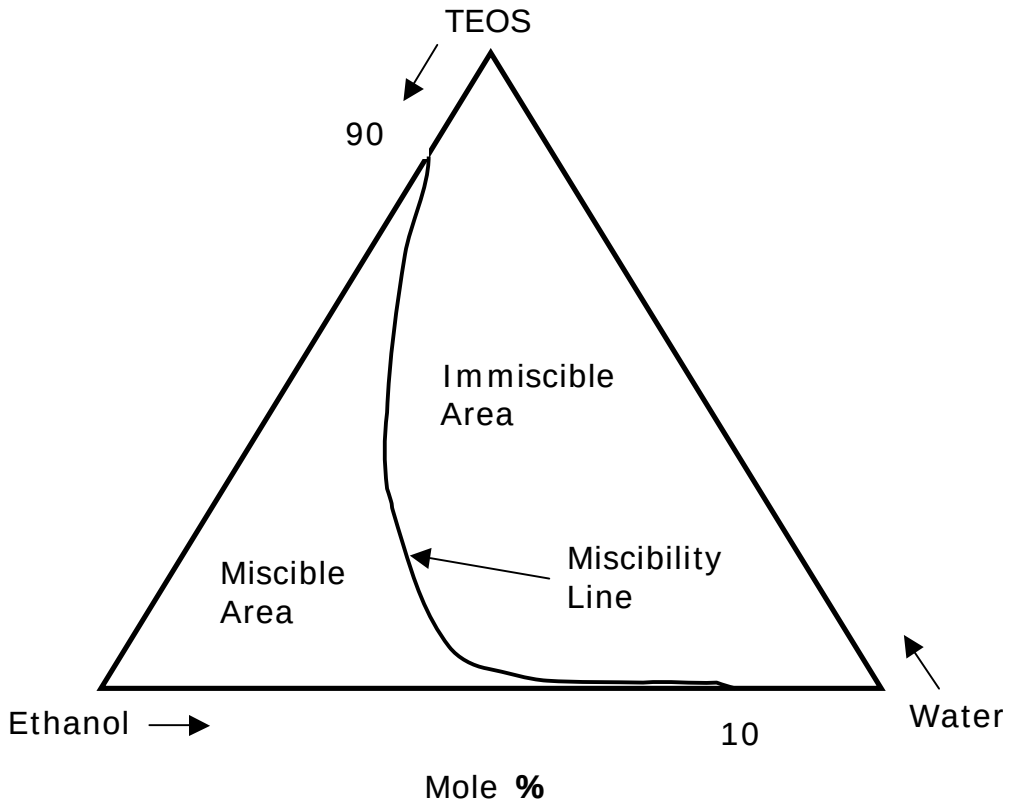

Figure 1.3.3.1: Ternary-phase diagram depicting miscibility of Sol-Gel precursors [16]

The effects of the relative amounts or concentrations of precursors are summarized in figure 1 above, adapted from Brinker and Scherer's text Sol-Gel Science [16]. Jones [19] has a similar diagram in his text and suggests that addition of an acid skews the miscibility line a lot closer to the TEOS – H_2O line. Other significant factors affecting the microstructures and gel times are temperature, the molar ratio of water to silicon (R) and the nature and concentrations of the precursors. These factors dramatically affect the relative rates of hydrolysis and condensation which dictate the pore sizes in the gel. Their effects will be discussed in the subsequent paragraphs.

1.3.3.2 Effect of R

The effect of the water content has been studied by several researchers for several precursors. Klein [20] has provided the most concise overview of the water content in conjunction with the other precursors. She identified three primary applications of the sols as coatable, castable and spinnable. Coatable sols contain less than 40 mole% of water and are ideal for making films; castable sols contain 40-70 mole% water and are ideal for making bulk monoliths while spinnable sols contain more than 70 mole% water. Figure 1.3.3.2 summarizes her findings.

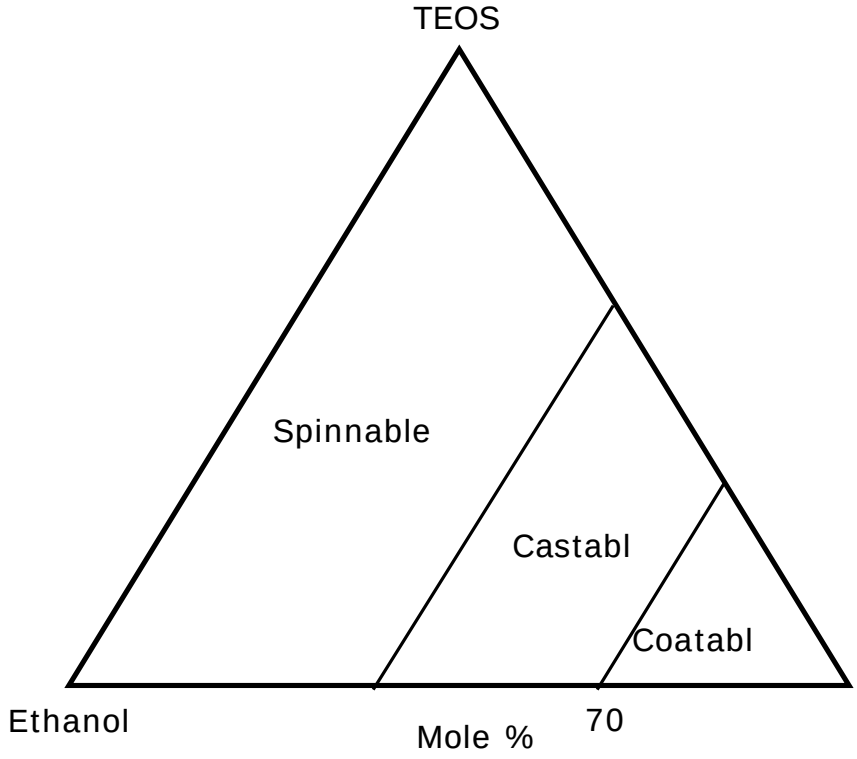

Figure 1.3.3.2: Effect of Water content on gel application

In the figure above, Brinker and Scherer also report that increasing R, the mole ratio of water to TEOS would increase the rate of hydrolysis and decrease the rates of condensation regardless of the pH. Klein used R to alter the amount of time it took to reach the gel point. Her optimum R ranges between 4 and 10. Optimum mole ratios near unity were reported for TEOS to ethanol ratios for minimal processing time. Two other factors of critical significance to the processing time and nature of the gels are temperature and the type(s) of catalyst(s) used.

1.3.3.3 Effect of Temperature

In addition to in-house experiments, which found the processing temperature to be a critical factor in controlling sol-gel processing time, extensive research [21, 22, 23, 24] have been reported to emphasize and further explain its effect on the resulting microstructures in addition to the processing time. Colby et al. [23, 24] found, among other things, that an increase in processing temperature leads to higher bulk densities and finer microstructure in the gels produced. Subsequent reports by the Colby's group studied the effects of processing temperature on characteristics such as surface area, average pore diameter and porosity of the gels. Their findings suggested a decrease in magnitudes of these properties as the temperature was increased.

1.3.3.4 Effect of Catalysts

The effect of catalysis on sol-gel processing is very profound; it is widely accepted that catalysts by definition increase the rates of reaction by providing alternate reaction pathways of lower activation energy. An additional stipulation is that they do not manifest themselves chemically in the final products of the reactions they catalyze. In sol-gel processing the catalysts manifest themselves physically in the final structure of the gels. Catalysis has been found to be necessary for timely hydrolysis but not for condensation [16]. What is of interest is that both hydrolysis and condensation can proceed with either acid- and/ or base-catalyzed reactions. As mentioned before, selection of the catalysts dictates the nature of the gels.

Hydrolysis, in acid catalyzed reactions, proceeds with an electrophilic attack of the hydronium ion on the tetraalkoxysilane. This draws the electron density away from the silicon atom rendering it with a partial positive charge. The electronegative water molecule attacks the charged silicon and acquires its charge thus making the protonated alkoxide a better leaving group. Leaving groups are atoms or radical groups that break away from an organic compound. Base catalyzed hydrolysis on the other hand proceeds by a nucleophilic attack on the tetraalkoxysilane by the hydroxyl ion, this subsequently weakens and displaces the '-O-C_nH_{2n+1}' groups. The results for both reactions are as depicted in Equation 1.3.2.3.

One of the most widely accepted proposed mechanism for acid- and based- catalyzed condensation involve either pentacordinate or

hexacordinate intermediate states, Brinker and Scherer go into further detail [14]. The isoelectric point of silica ranges between pH = 1.5 - 2. Below the isoelectric point, silanol groups get protonated and above it they get deprotonated. However, when the pH is about neutral, significant amounts of both protonated and deprotonated silanols are present. The rate of condensation is believed to be maximized when the pH is neutral.

From the preceding, it follows that for acid catalyzed sol-gel reactions, condensation usually ends before hydrolysis. This is because the lower pH leads to faster and excessive hydrolysis while retarding the rates of condensation. The relative rate of the hydrolysis reaction is much higher than that of the condensation reaction. This yields gels with smaller pore sizes and higher densities which are a result of highly linearized polymer molecules with minimal branching. Since the capillary forces vary inversely with pore size, acid catalyzed gels are more prone to cracking during the drying stages of sol gel processing.

In contrast, for base-catalyzed reactions the higher pH leads to the relative rates of reactions favoring condensation. The faster condensation rates result in gels having larger pore sizes which are less likely to crack during the drying phases of sol-gel processing.

Chapter 2 Experimental Materials, Equipments and Procedures

2.1 Sol-Gel Processing - Materials

Several processing techniques and recipes were attempted. As all the recipes employed were from publications, excluding a couple that was obtained from individuals with extensive proficiency on sol-gel processing; the following is a review of the sources and properties of the materials used. Though they varied only slightly, their effects were very remarkable, as was to be expected, given the individual and combined effects of the factors addressed in the previous chapter. Each recipe consisted of chemicals that provided a source for silicon and water which are the primary reactants and a homogenizing medium for the reaction to occur – an alcohol. An acid or base catalyst and in some cases both are used to speed up the reactions. Some recipes required other additional materials, additives, which are also listed.

2.1.1 Reactants: Silicon and Water Sources

Two primary sources of silicon were utilized in experimentation, tetramethylorthosilicate – TMOS and tetraethylorthosilicate – TEOS. Earlier researchers focused on TMOS for silicon, over the years however, TEOS has increasingly become the favorite of the two. They are both equally effective however, the former is significantly more expensive than the latter; as such, most of this study utilized TEOS as the primary source for silicon. Also the use of both chemicals required extreme care for safety but TMOS was a little more toxic. No modifications were made to the chemicals and were used as received.

Tetramethylorthosilicate (TMOS)		
Supplier	Sigma-Aldrich	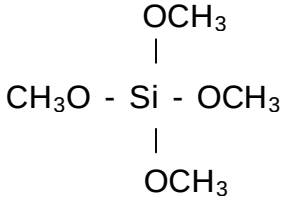
Empirical Formula	$C_4H_{12}O_4Si$	
Molecular Weight (g/mol)	152.22	
Density (g/cm^3)	1.032	
Purity	99+%	

Additives used in some experimentation methods could be considered as sources of silicon but their quantities were too minute to be listed as such.

Tetraethylorthosilicate (TEOS)		
Supplier	Fisher Chemicals	
Empirical Formula	$C_8H_{20}O_4Si$	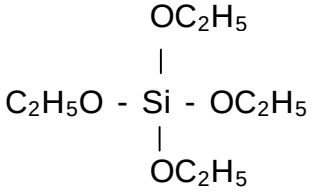
Molecular Weight (g/mol)	208.34	
Density (g/cm^3)	-	
Purity	98.0	

Type I reagent grade water (H_2O) was obtained fresh from a Barnstead Water System which provides the following specification for the processed water.

Type I Reagent Grade Water (H_2O)		
Supplier	Barnstead Water Systems	
Empirical Formula	H_2O	
Molecular Weight (g/mol)	18.02	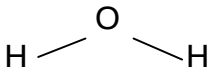
Density (g/cm^3)	1	
Purity	<3ppb TOC, <0.02 Eu/cm^3 endotoxin	

2.1.2 Homogenizing Agents

Two homogenizing agents corresponding to the silicates sources above were necessary to provide a common medium for the hydrolysis and condensation reactions to occur. Pajonk et al [25] also report that transesterification is avoided by doing so. These were also used as received.

Methanol (MeOH)		
Supplier	Aalder Alcohols	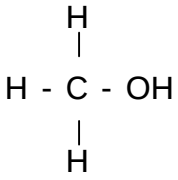
Empirical Formula	CH_4O	
Molecular Weight (g/mol)	32.04	
Density (g/cm^3)	0.791	
Purity (%)	100	

Ethanol (EtOH)		
Supplier	Aalder Alcohols	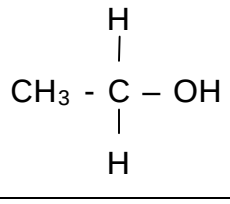
Empirical Formula	C_2H_6O	
Molecular Weight (g/mol)	46.07	
Density (g/cm^3)	0.785	
Purity (%)	100	

2.1.3 Catalysts

Several catalysts were utilized, the basis of their use were predetermined by the publications from which the recipes were obtained. Some of them were used as received while others were modified to meet the specified pH and concentrations. As a reminder, the catalysts were used in one of three formats for each processing technique; the formats are Single-Step Acid, Single-Step Base, and Two-Step Acid-Base. So for the single-step acid and the two-step acid-base recipes, the acid catalyst used is HCl. Received as shown the modified per recipe for experimentation by the appropriate dilution.

Hydrochloric Acid (HCl)		
Supplier	E M Science	
Empirical Formula	HCl	
Molecular Weight (g/mol)	36.46	H - Cl
Density (g/cm^3)	1.190	
Purity (%)	37.25	

While for the single-step base and the two-step acid-base recipes, the base catalyst used is NH_4OH. Ammonium hydroxide is received as shown, then modified per recipe for experimentation by the appropriate dilution.

Ammonium Hydroxide (NH_4OH)		
Supplier	Fisher Chemicals	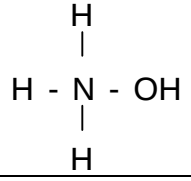
Empirical Formula	NH_4OH	
Molecular Weight (g/mol)	35.03	
Density (g/cm^3)	0.90	
Purity (%)	29.3	

2.1.4 Additives, Buffers and Other Chemicals

Additives are chemicals introduced during specific phases of the sol-gel process to help prevent or confer some level of control on the gel structure and integrity.

Methoxytrimethylsilane (MTMOS)	
Supplier	Sigma-Aldrich
Empirical Formula	$SiC_4H_{12}O$
Molecular Weight (g/mol)	104.23
Density (g/cm^3)	0.759
Purity (%)	99

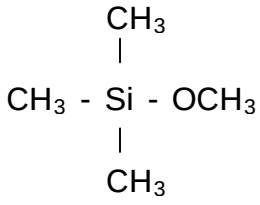

n-Heptane was introduced during the second washing phase of Einarsrud et al sol-gel processing recipe. It was used as received.

n-Heptane (C_7H_{16})	
Supplier	Sigma-Aldrich
Empirical Formula	C_7H_{16}
Molecular Weight (g/mol)	100.21
Density (g/cm^3)	0.683
Purity (%)	99

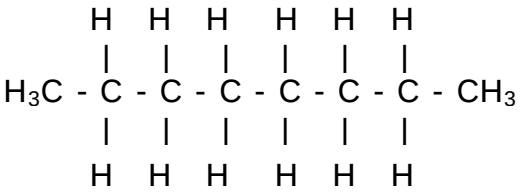

Ammonium Fluoride is used as a buffer for the single-step base catalyzed reaction. It was modified to meet the specification of the said reaction.

Ammonium Fluoride (NH_4F)	
Supplier	Fisher Chemicals
Empirical Formula	NH_4F
Molecular Weight (g/mol)	35.03
Density (g/cm^3)	0.90
Purity (%)	29.3

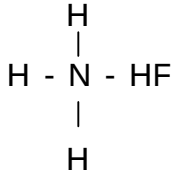

Oxalic acid is required in one recipe a little difficult to classify because it acts, not only as a catalyst, but also as a drying-chemical control agent [22]; for this reason it was listed under “other chemicals”.

Oxalic Acid ($C_2H_4O_2$)		
Supplier	Aldrich	OH
Empirical Formula	$C_2H_4O_2$	|
Molecular Weight (g/mol)	90.04	O=C - C =O
Density (g/cm^3)	1.9	|
Melting Point (^{o}C)	157	OH

Commercial silica gel powder was used for the strengthening of the preforms as exemplified by Okazaki et al. In addition Silica gel powders obtained from grinding home-made monoliths were also used but not concurrently. Below are the listed specifications of the commercial silica gel.

Silica Gel Powder (SiO_2)		
Supplier		| | |
Empirical Formula	SiO_2	- Si – O – Si – O – Si -
Molecular Weight (g/mol)	90.04	| | |
Density (g/cm^3)	1.9	- Si – O – Si – O – Si -
Mesh size	157	| | |
		- Si – O – Si – O – Si -
		| | |

2.1.5 Critical Drying Fluid

Carbon dioxide (CO_2) is the drying fluid utilized in the critical point drying operation to make aerogels. It is supplied as dry liquid carbon dioxide in a siphon cylinder.

Dry Liquid Carbon Dioxide (CO_2)		
Supplier	Holox Inc.	
Empirical Formula	CO_2	
Molecular Weight (g/mol)	44	
Critical Pressure (psi)	1100	O = C = O
Critical Temperature (^{o}C)	31.5	

2.2 Sol-Gel Processing - Equipment

Sol-gel processing is a fairly low-tech process that requires simple equipment to be performed. However, things get a little intricate once critical point drying and characterization of the gels commence.

2.2.1 Glassware, Heating, Stirring and Measuring Equipment

Glassware utilized includes beakers, graduated cylinders, Petri-dishes and pipettes. For very accurate measurements of small quantities, Finnpipette® pipettes were used to reduce error. A Corning hot plate/stirrer with magnetic stirrers was used for heating and stirring contents of the reactor beakers. A sand bath was used for more accurate temperature control while the temperature was read off a mercury thermometer. The pH of the reaction was determined with the Corning 455 Ion Analyzer/pH meter. A schematic of the experimental setup is provided below.

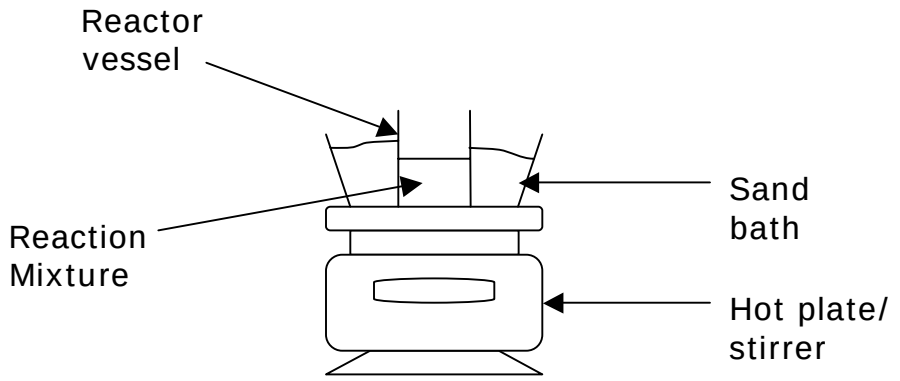

Figure 2.2.1.1: Schematic of reactor setup. Parafilm, thermometer and magnetic bar stirrer not shown

2.2.2 Critical Point Drying Equipment

The E3100 Polaron Critical Point Dryer manufactured by Quorum Technologies was used in conjunction with a ThermoNeslab RTE 7 heater/chiller unit for the solvent exchange and the subsequent supercritical extraction of carbon dioxide. The former provides the

pressure chamber capable of enduring the critical pressure while the latter provides a means of controlling the temperature of the chamber by circulating water through a water jacket which surrounds it.

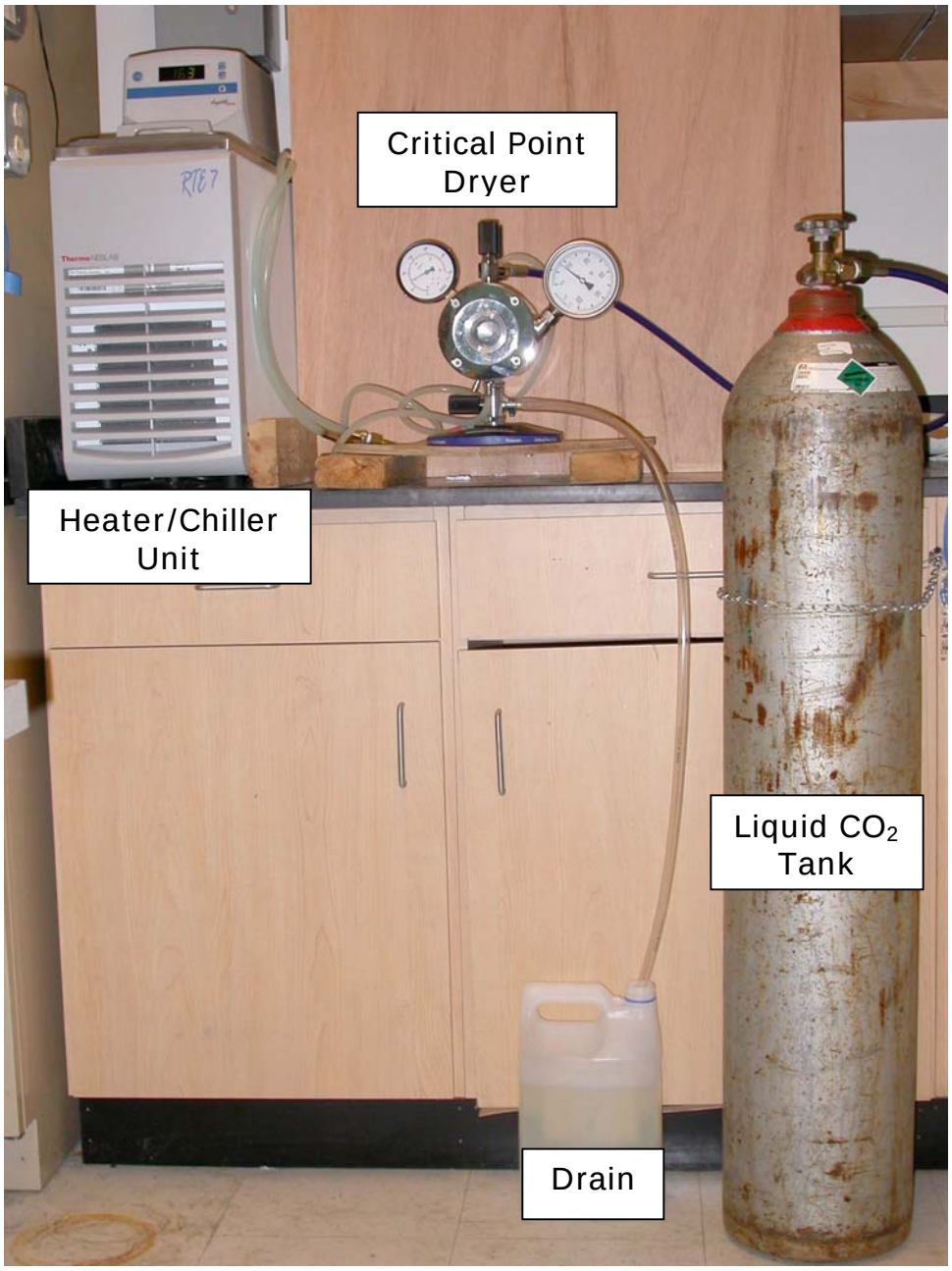

Figure 2.2.2.1: Critical Point Dryer and Heater-Chiller System connected to Drain and CO_2 tank

2.2.3 Sol-Gel Characterization Equipment

Scanning electron microscopy (SEM) was used to study the surface morphology of the gels at very small scales. Prior to this, the samples

were coated with a thin film of gold to dissipate the electron beam energy to eliminate excessive charging. Gold coating was done with a sputter coater while the SEMs were taken with a LEO 1550 Ultra High Emission SEM.

The percentage of porosity was determined from the skeletal density and bulk density by calculating the fractional difference in density; more detail will be provided at a later time. The skeletal density was obtained by helium pycnometry with the Micromeritics, AccuPyc 1330 pycnometer while the bulk density was determined by Archimedes principles using a set-up provided by Mettler-Toledo electronic scales.

2.3 Sol-Gel Processing - Procedure

Several procedures were attempted during the early stages of the project. With time and consulting with Scott Reed, a research associate with Sandia National Labs and complementary input by Ashley White, alumnus of the Lawrence Berkley National Labs Summer Research Program, two primary methods were identified. The next few paragraphs will describe the procedures of these two recipes or procedures and others of particular interest. Each procedure generally consists of the following steps:

(i) Hydrolysis and condensation: the order in which reactants are introduced has a profound effect on the final gel so this will be addressed on a case-by-case basis

(ii) Casting: this was the physical pouring of the sols into the designated molds just before the gel points are reached

(iii) Gelation: is characterized by an abrupt or gradual but significant change in the viscosity of the sols; the gel times and relative speeds of gelation will be addressed as necessary

(iv) Aging: specific conditions also varied slightly for the different recipes will be addressed accordingly; it usually consisted of keeping the gel in its pore liquid or alcohol at a fixed temperature for set periods of time

(v) Washing: was specific to some recipes and involved the rinsing of the gels in alcohol baths daily for set periods of time

(vi) Drying: for aerogels, the samples are processed through critical point drying and to make xerogels, the gels were either heated according to specific temperature profiles or sealed in molds with parafilm and left on isolated shelves; holes were poked into the parafilm seals on a bi-monthly basis to control the rates of evaporation, and finally,

(vii) Densification: is simply an extension of the temperature profile beyond the drying temperatures to allow the gels to approach the properties of fused silica.

These steps were followed by a series of characterization techniques to be elaborated upon at a later time.

2.3.1 Sandia National Labs Procedure: 2-Step Acid-Base

This procedure was obtained while consulting with Scott Reed, by way of The Los Alamos National Labs in New Mexico, so naturally it follows the acid-base catalysis preparation format outlined by Brinker et al [26]. The advantage of the two-step process is that it eliminates any effects of phase separation and precipitation and has a finer control of both the hydrolysis and condensation rates of the sol-gel reactions. The first step comprises making a stock solution by mixing specified amounts of the reactants and the acid catalyst at 60^{o}C. For the second step, freshly made ammonium hydroxide is added to this solution after an hour and thirty minutes. Gelation usually occurs within 10 – 30 minutes at 60^{o}C after the addition of the base. The overall mole percentages for the reactions are shown in the table below. For a more complete listing of the recipe, please refer to the Appendix A.

Chemical	Mole Percent
TEOS	17.43
Ethanol	64.94
HCl	0.01
H_2O	17.41
NH_4OH	0.21

Aging of the 'Sandia recipe' was processed in an ethanol bath container in which the parafilm sealed molds were placed. This setup was place in an explosion-proof oven at 50^{o}C.

2.3.2 Lawrence Berkeley National Labs Procedure: Single-step Base

This recipe was obtained through discussions with Ashley White, by way of the Lawrence Berkeley National Labs in Berkeley, California. It differs slightly form most other single-step base catalyzed procedures by the sequence of mixing of the reactants. The TEOS is first mixed with ethanol in one beaker and in the other beaker, is a mixture of water, the catalyst – ammonium hydroxide, and the buffer –

ammonium fluoride. The mole percentages of reactants were TEOS 2.74, 10.21, 86.99, 0.05, and 0.01% for TEOS, ethanol, water, ammonium hydroxide and ammonium fluoride respectively.

Chemical	Mole Percent
TEOS	2.74
Etanol	10.21
H_2O	86.89
NH_4F	0.05
NH_4OH	0.02

The contents of these beakers are subsequently mixed into the reactor vessel to start the hydrolysis reaction. The original recipe required that the mixture is left to sit until gel point was reached after a brief spell of stirring. This took in excess of 11 hours for gelling to occur. The recipe was modified to reduce the processing time by following Taguchi's principles for design of experiments.

The primary factors identified for variation were the process temperature, and the amounts of catalyst and buffer solution used. Each factor was varied at three levels so an L-9 orthogonal array was used to study the process. Upon analysis of the data collected, temperature was found to be the most critical to reduce process time followed by the amount of buffer solution then the amount of catalyst. This was confirmed and was utilized. The table below shows the final recipe used at a process temperature of 60^{o}C.

After the gel was obtained, they were sealed in an ethanol bath while still in the molds for a day. On the second day the gels were carefully removed and placed in a fresh ethanol bath. The gels were washed daily with new ethanol baths for two or more days before drying was initiated in a critical point dryer or at ambient temperature and pressure.

2.3.3 Wang Procedure: Single-Step Acid

Wang's procedure, by way of University of Florida, was adapted from his doctorate dissertation for its claims of tailoring the pore sizes of the gels. Unlike most other recipes, this one required use of TMOS as the source for silicon and a total of only three ingredients, no homogenizing agent, were used. The oxalic acid doubles as a catalyst and a drying control chemical additive, DCCA. Following casting gelation after a few hours, the gels were aged at ~ 75^{o}C for 24 – 48

hours. Drying was achieved following a drying profile for most samples and also by supercritical extraction for other samples.

Chemical	Mole Percentage
TMOS	5.68
H_2O	93.95
Oxalic Acid	0.37

2.4 Sol-Gel Processing - Characterization

The optical fiber performs are characterized by scanning electron microscopy, porosimetry, ellipsometry and infrared spectroscopy. These characterization methods reveal the surface morphology, porosity, optical properties and chemical integrity of the preforms respectively.

2.4.1 Scanning Electron Microscopy

The surface morphology characterization of the gels at very small scales was achieved by scanning electron microscopy (SEM). The microscope chamber was evacuated to create a vacuum and highly focused electron beams were swept across the entire sample. The scanning electron micrograph is an interpretation of the secondary electrons and x-rays emitted by the sample.

Due to the high porosity of the gels, the air trapped inside the pores are extremely susceptible to charging which causes image drifting once they are bombarded with energy. Excessive charging is primarily minimized by coating the gel samples with thin films of gold to dissipate the electron beam energy. This can however be aided by mounting the gel samples with silver paint during the sample preparation as opposed to directly onto carbon tape. In some cases however, the silver paint peels off the mount so carbon tape was used to secure it to the mount.

2.4.2 Porosimetry

The porosity of the gels can be obtained in various manners. The most predominant being N_2 adsorption followed by surface area calculation using the five point Brunauer, Emmett and Teller (BET) theory and the use of Helium pycnometry to determine the skeletal

density [22,27,28,29]. The bulk densities of the gels were often determined by Mercury pycnometry.

A less sophisticated, and less expensive, but effective method was used in determining the porosity of the gels produced. Like most other researchers, the Helium pycnometer was used to determine the skeletal density of the gel but the bulk density was determined by Archimedes' principles, a method adapted from Rao et al [30]. The percentage porosity, P_r is calculated from the values of the skeletal density, ρ_s and the bulk density ρ_b using the relation in equation 2.4.2.1:

$$P_r = (\rho_s - \rho_b)/\rho_s$$

Equation 2.4.2.1: Relation for determining the percentage porosity, P_r

Chapter 3 Results and Discussions

3 Results

Ideally the expected results for this project would have included samples of random hole optical fibers drawn out from preforms fabricated by sol-gel processing. Samples of aerogels were hand-drawn to demonstrate their feasibility as a suitable cladding material.

A majority of the initial focus of the study was devoted to understanding sol-gel processing and the ability to tailor the porosity of the resulting glass. This was followed by the fabrication of xerogels whose recipes were drawn from a wide array of literature. The following sections will review and discuss the results of xerogels then aerogels and comment on their suitability for fiber drawing using previous attempts as a reference. Experiments on optimizing various stages of sol-gel processing as well as characterization of the gels will also be reviewed and discussed.

3.1 Hand-Drawn Aerogel Samples

Preliminary fibers were hand-drawn from some of the gel samples using a gas-oxygen torch. The xerogels were tougher to draw than the aerogels; this was probably because they may have contained remnants of pore fluid within their structures. The xerogels used were derived from Sakka and Kamiya [34]. Aerogels drawn here were derived from the Berkeley recipe and heat-treated to 800^{o}C before fiber drawing with the flame gun. It got progressively easier to hand-draw fibers from aerogels that were heat treated to higher temperatures.

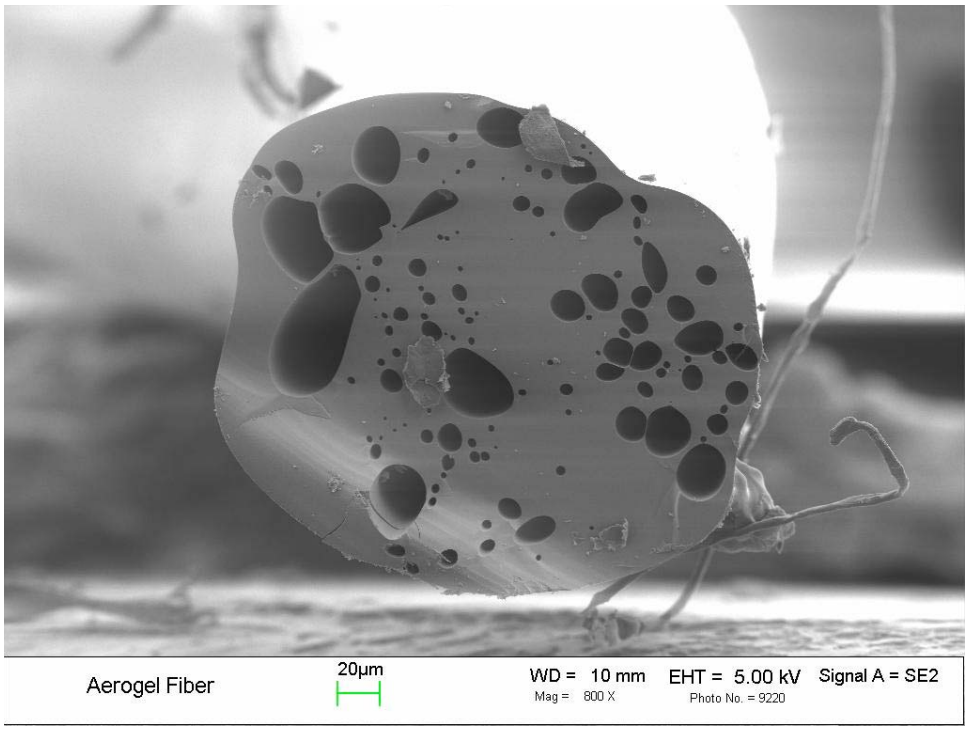

Figure 3.1.1: Hand-Drawn Aerogel

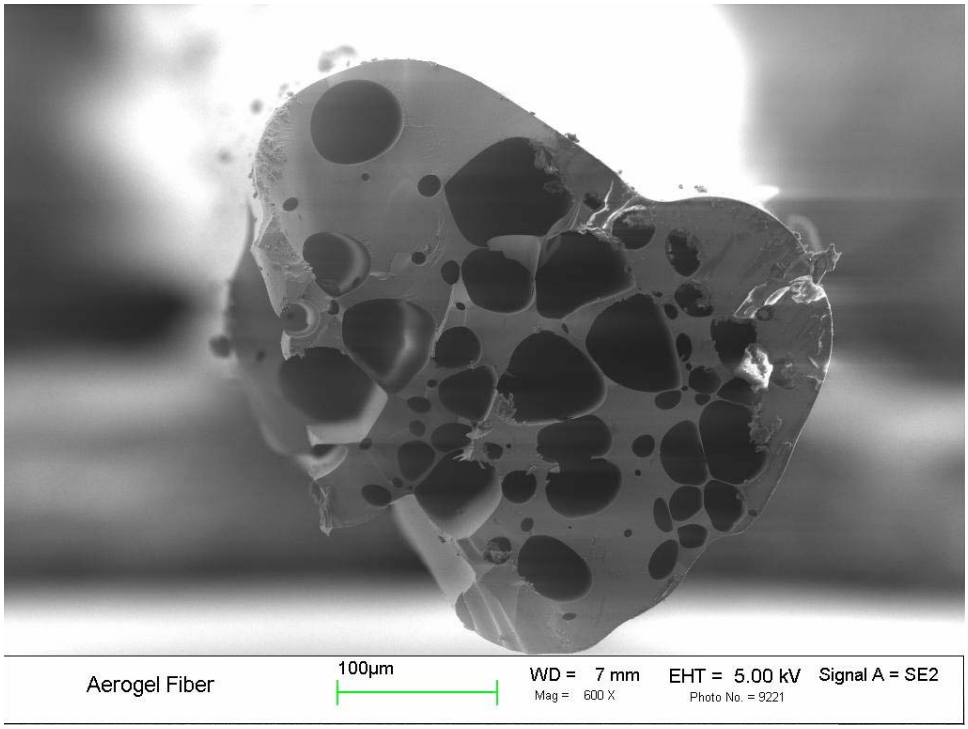

Figure 3.1.2: Hand-Drawn Aerogel

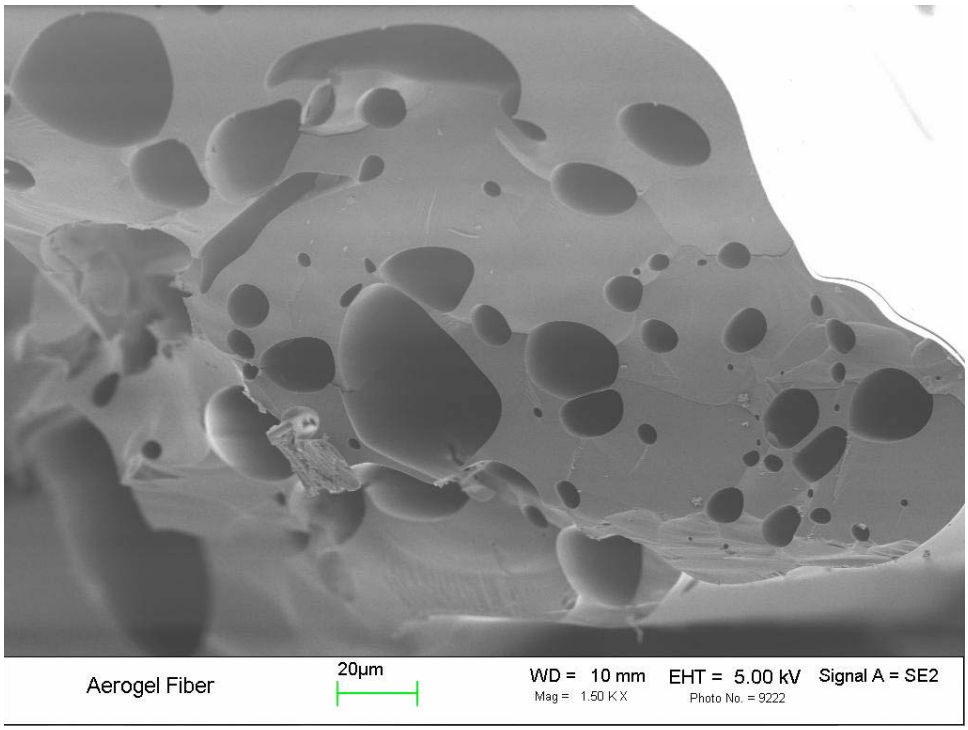

Figure 3.1.3: Hand-Drawn Aerogel

The SEM micrographs show the random distribution of holes in the hand-drawn aerogels. It follows that sol-gel processing can be used to fabricate preforms for manufacturing the cladding of random hole optical fibers.

3.2 Pictures of Gels

The pictures displayed are representative samples of aerogels and xerogels fabricated. The xerogels are dense and compact with no visible porosity. These may be too dense and may not be useful as cladding material in the random holey fibers.

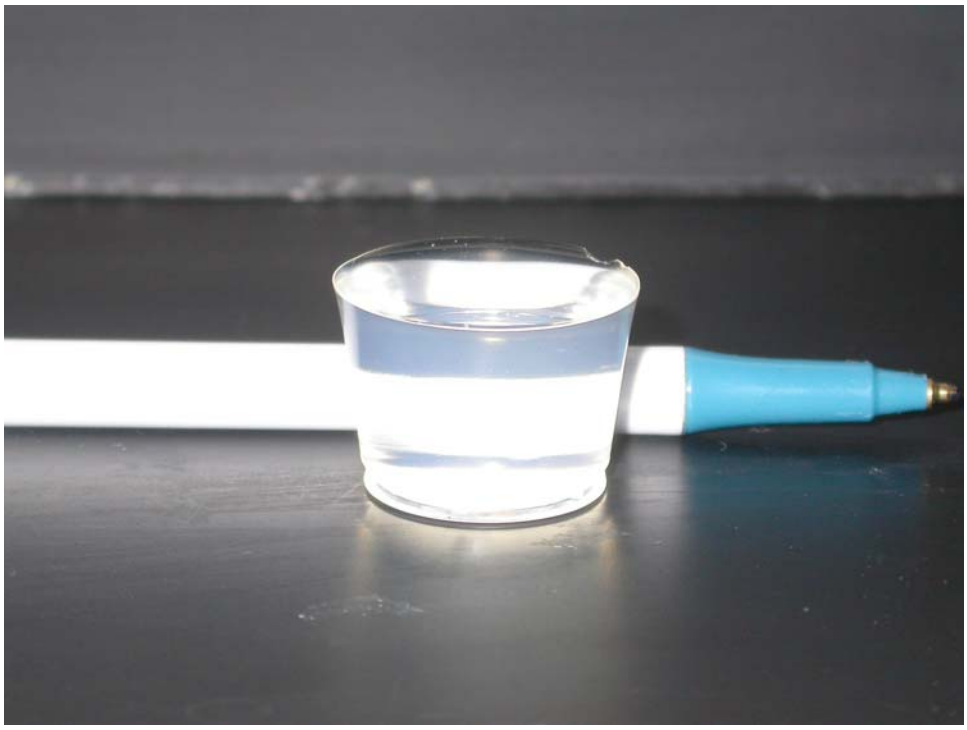

Figure 3.2.1: Sandia Xerogel after several months of ambient temperature and pressure drying

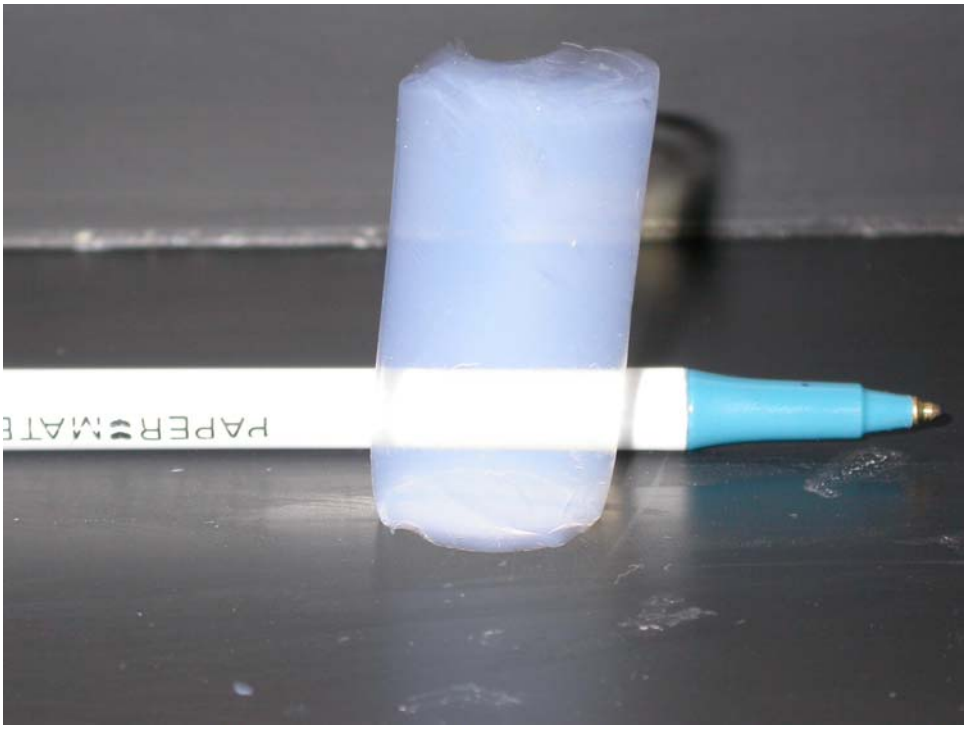

Figure 3.2.2: Sandia Aerogel after 3 days of critical point drying

The aerogel shown in figure 3.2.2 may be better suited for the cladding because of its visibly higher porosity. However if the porosity

is too high, the physical structures have been known to wither away when subjected to the high temperatures during fiber drawing in the draw tower. Using aerogels with varying porosities and/or pore sizes may reveal the ideal characteristics of the gel required for adequate average indexing behavior.

3.3 Scanning Electron Micrographs (SEM) of Gels

Several researchers have reported methods of densification by using temperature profiles. The degrees of densification were somewhat related to the temperatures to which the gels were exposed and how long they were held at these temperatures. Several samples of aerogels fabricated by the Lawrence Berkeley National Labs recipe were processed through the temperature profiles shown below and samples were removed at each holding temperature and characterized with scanning electron microscope. All the micrographs were taken using the InLens camera with the EHT at 5.00 kV and the Inlens was at a variable working distance between 3-5mm. The magnification of the samples was 100.00 kX and the scale for each sample is displayed on the micrograph.

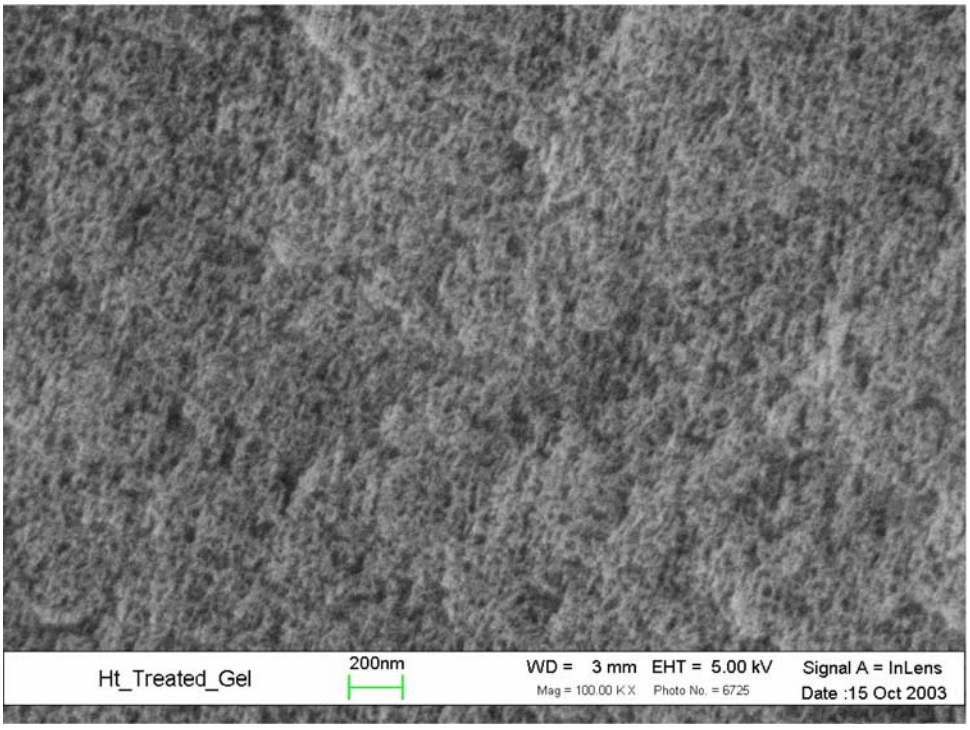

Figure 3.3.1: SEM of Berkeley Gel sample heat treated at 60^{o}C

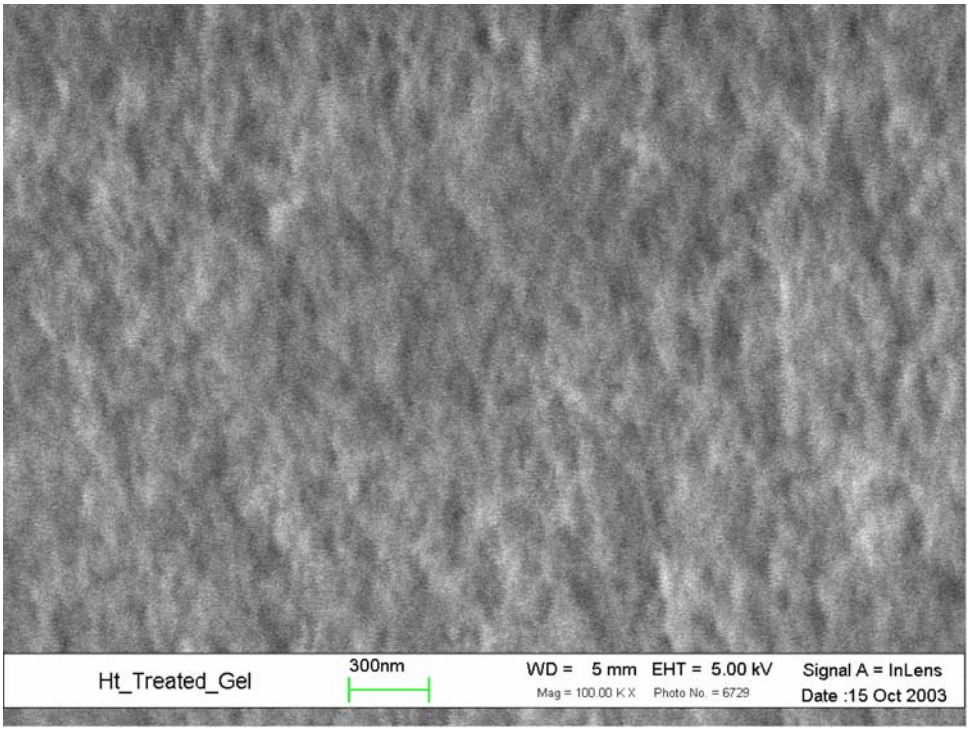

Figure 3.3.2: SEM of Berkeley Gel sample heat treated at 350^{o}C

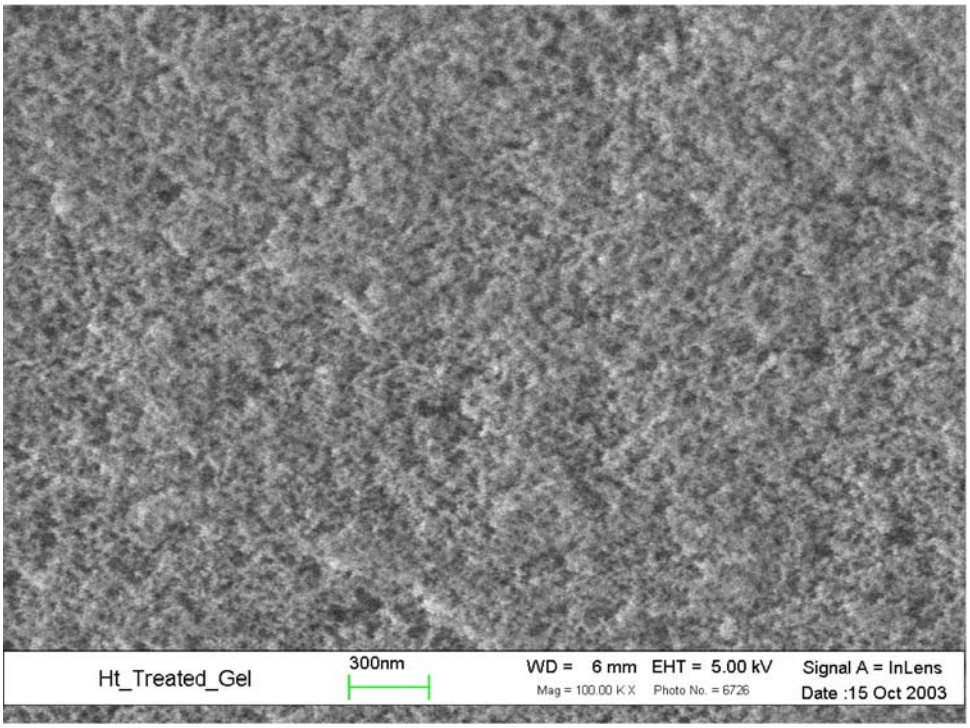

Figure 3.3.3: SEM of Berkeley Gel sample heat treated at 400^{o}C

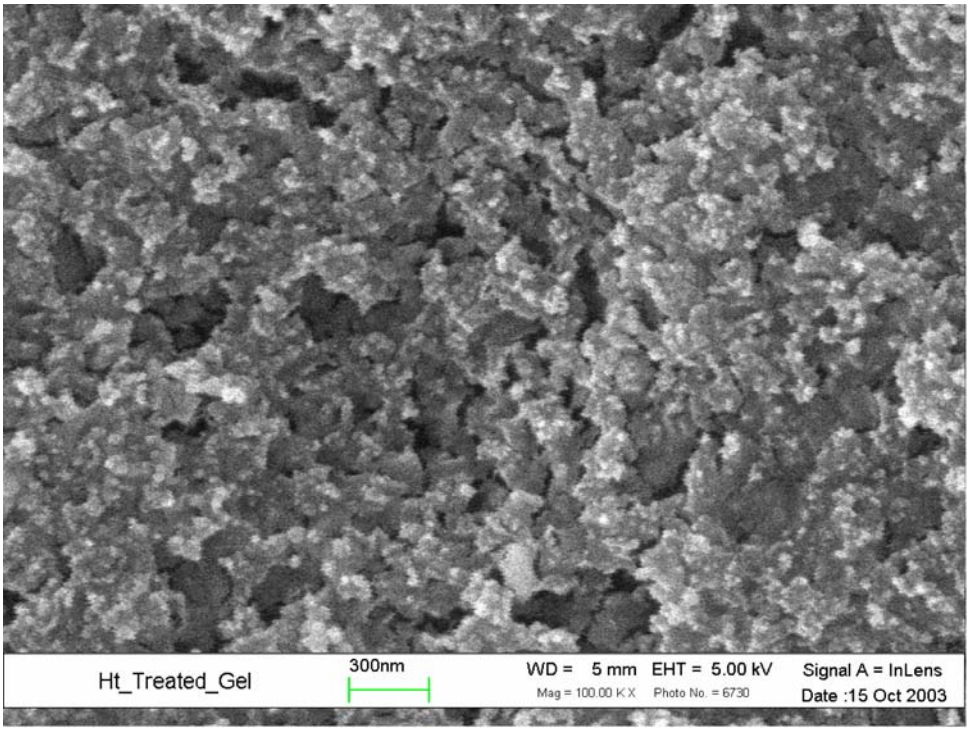

Figure 3.3.4: SEM of Berkeley Gel sample heat treated at 600^{o}C

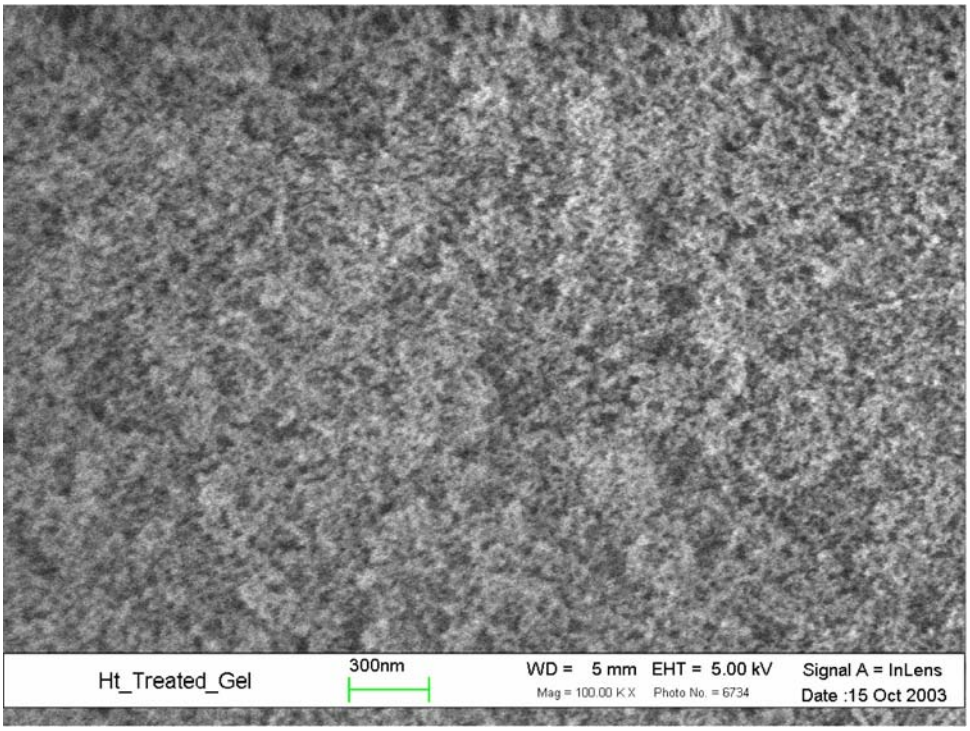

Figure 3.3.5: SEM of Berkeley Gel sample heat treated at 700^{o}C

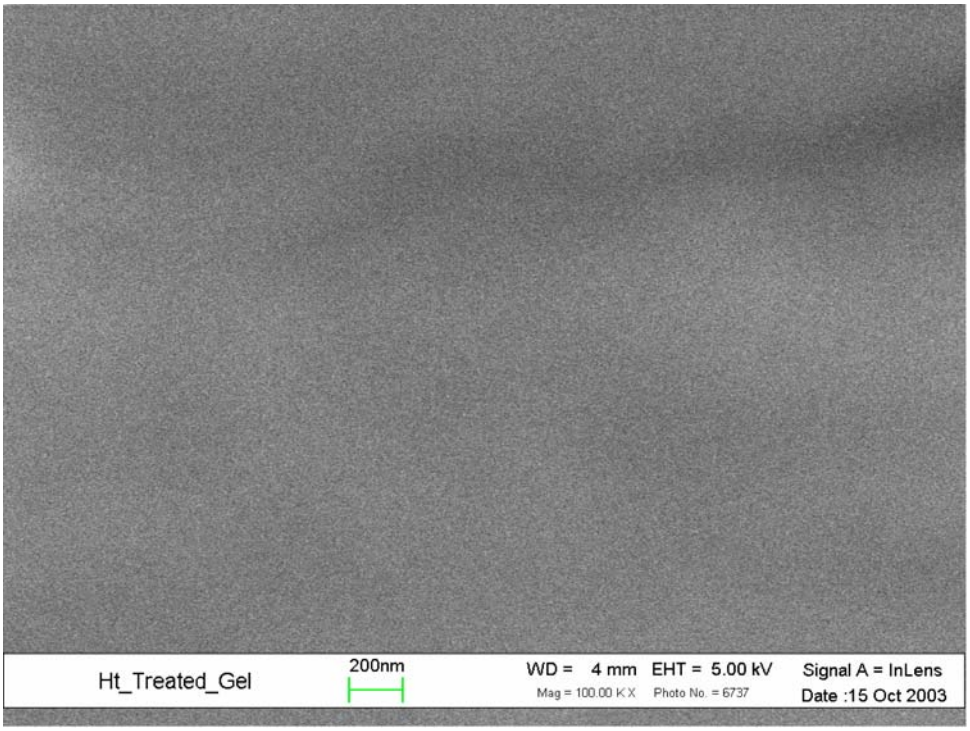

Figure 3.3.6: SEM of Berkeley Gel sample heat treated at 800^{o}C

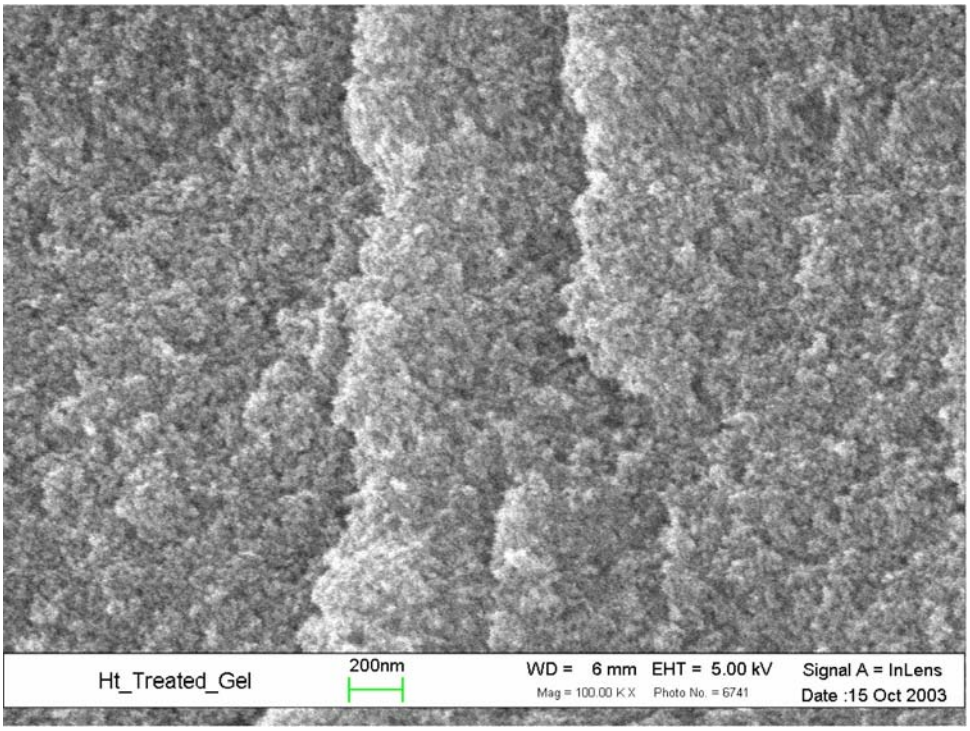

Figure 3.3.7: SEM of Sandia Gel sample heat treated at 60^{o}C

The reason for taking the SEMs was to track the physical changes in the appearance of the gels and the structure of the pore sizes as well. Although trends seem to be obvious densification of the gel samples

with increasing temperature, a more definitive analysis is required to confirm these observations. Also noteworthy is the significant difference in the pore sizes, pore size density and general appearance of figure 3.3.1 and figure 3.3.7 which correspond with the Berkeley and Sandia recipe gels respectively both after equivalent heat treatment cycles at 60°C. The pore sizes in the Berkeley gels (base catalyzed) appear much smaller than the Sandia gels (both acid and base catalyzed.) Again these observations can be better quantified upon further nitrogen adsorption analysis.

3.4 Helium Pycnometry

Rao et al [30] used helium pycnometry as an alternative method of determining the skeletal density of aerogels. However this method could not be extensively used in this study primarily because the samples wouldn't always sink readily onto the scales when they were being weighed in the fluid -- both water and ethanol were tested. Nevertheless some data was collected for corresponding samples previously observed in the SEM.

Gel Recipe	Weight (g)	Temperature (°C)	Skeletal Density (g/mL)	Standard Deviation (g/mL)
Sandia	0.1644	60	1.6595	0.004
Berkeley	0.0713	60	2.0186	0.0086
Berkeley	0.0655	600	2.1893	0.0258
Berkeley	0.0566	700	2.3653	0.0527

Due to the problems listed above, no data was obtained for the samples heat treated at 350, 400, 500 and 800°C. However the trends observed are consistent with those obtained in the SEMs. The unusually high density of silicon dioxide has also been observed, in commercial aqueous silica gels, by R.K. Iller and also noted by Brinker and Scherer [16]. The density of pure fused silica is about 2.2 g/mL.

3.5 Process Improvement by Design of Experiments (DOE)

After sampling dozens of recipes for sol gel processing the Berkeley recipe was favored because less complications were encountered during the supercritical extraction step. However the hydrolysis and condensation steps still took at least two hours to complete. To reduce the processing time, DOE techniques were employed.

The selected factors of primary importance were the process temperature, the amount of catalyst used and the amount of buffer solution used in the sol gel processing. Three factors for each level were examined using an L-9 orthogonal array in the experimental setup – see appendix for experimental design. Qualitek software designed by Nuteck, Inc. was used in the analysis of the data obtained; the results are as follows:

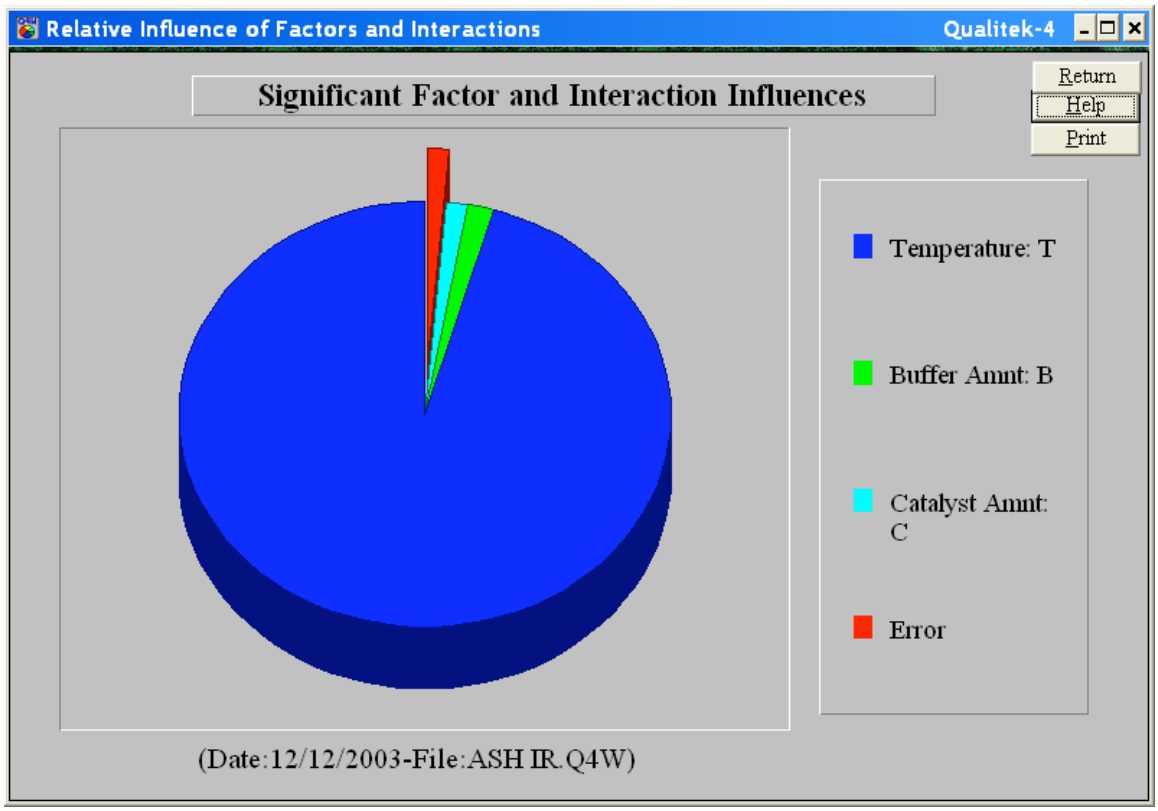

Figure 3.5.1: Screen Capture of Pie Chart Showing the Relative Influence of Design Factors

Figure 3.5.1 above shows the relative influence of each factor on reducing the sol gel processing time of the Berkeley recipe. Of them, temperature was found to have the greatest influence; the other factors are adjusted in accordance to the optimum settings suggested from the data as displayed in Figure 3.5.2 below.

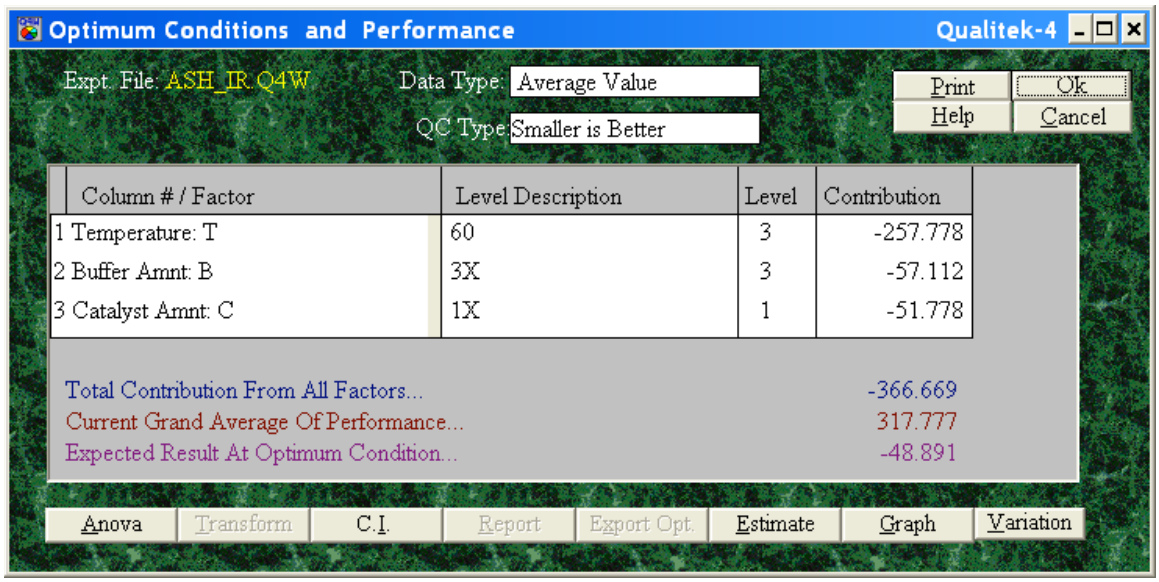

Figure 3.5.2 Screen Capture Showing Optimum Performance Conditions

The expected results are listed as -48.891 minutes however confirmation tests revealed the processing time to be reduced to just over 16 minutes from a previous time of over 17 hours. The DOE explanation suggested that temperature was the most significant of the factors studied. Hench and West [22], in "The Sol-Gel Process", suggests that the rate of hydrolysis increases appreciably with increasing temperature. Further reduction in processing time is induced by the buffer NH_4F which might have contributed more ammonium ions to ensure adequate amounts were present. The buffer also generates fluoride ions which have also been reported by [31] to reduce processing time.

3.6 Mechanically Induced Holes in Random Hole Optical Fibers

Another approach evaluated was the mechanical introduction of holes into a zerogel specimen. Thin nylon threads or coated fibers are introduced into the specimen while the samples are still in the sol-phase (inside the molds) of the process and carefully extracted after the gel-phase has been reached and surpassed.

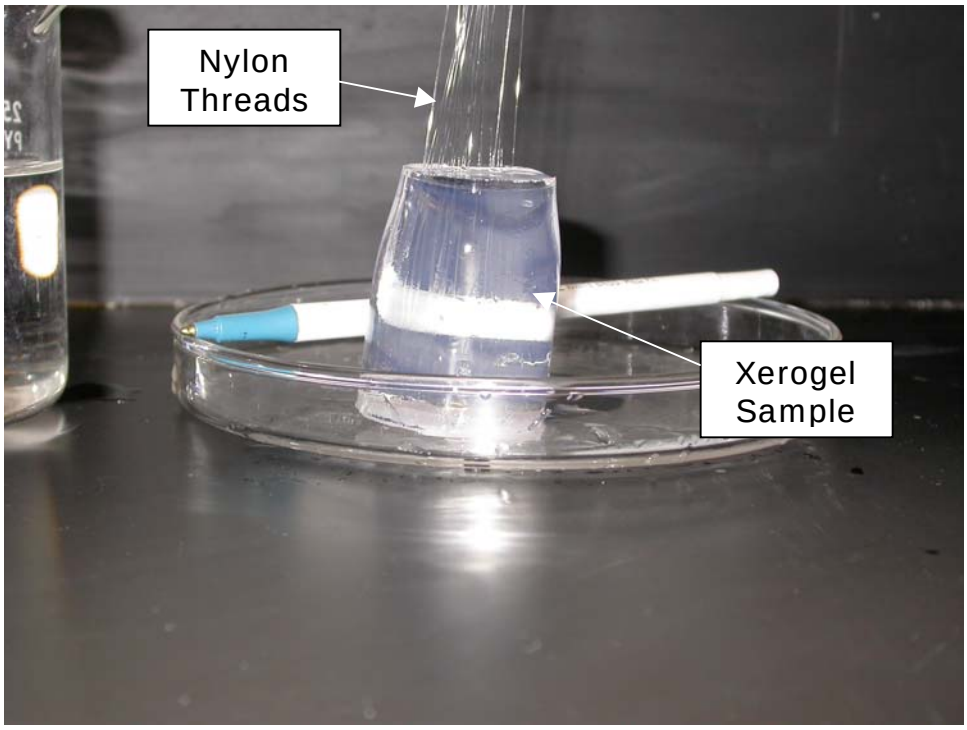

Figure 3.6.1: Xerogel with mechanically induced holes

This approach seems highly feasible and will be successful if foreseeable factors like shrinkage of the monoliths which will determine the sizes of the preforms as well as the holes, and drying rates or profiles which will determine the overall process time are carefully addressed.

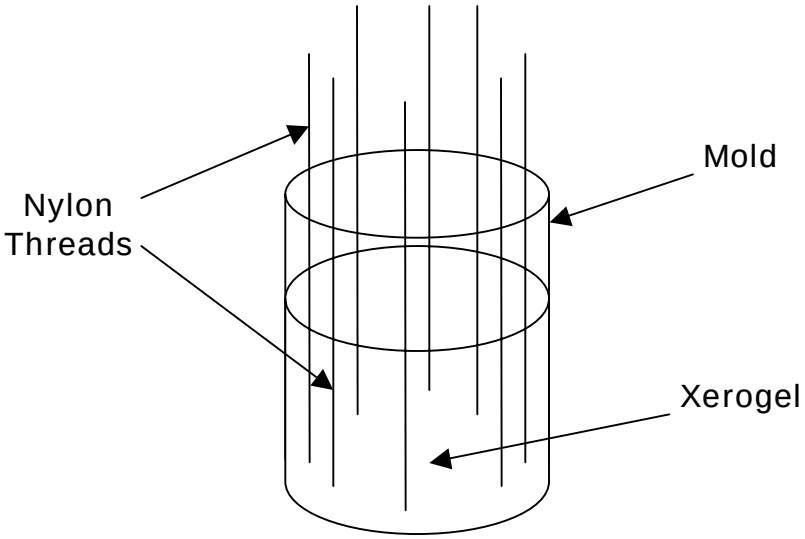

Figure 3.6.2: Schematic of Mechanically Induced Preform Setup

Chapter 4 Conclusions and Future Work

Aerogels appear to be too porous and while xerogels appear to be too dense to be effective means of manufacturing random holey fiber cladding materials. Aerogels may be densified by temperature treatment or other processing techniques to obtain ideal processing properties of the preforms for fiber drawing.

Cladding material for random hole optical fibers preforms were made by Sol-Gel processing. Aerogel samples of varying porosities achieved by utilizing heat treatment profiles to induce and promote drying and densification of aerogel. Treatment at higher temperatures over longer periods of time yielded gels with higher densities. It was progressively easier to draw gels that were treated to higher temperatures with the gas-oxygen torch. The distributions of pores in the hand-drawn fibers were comparable to those made by the previously mentioned GPP method.

Given the current progress of the experiments, it is imperative that research continues to completely realize the goals of the project, fiber drawing of sol-gel preforms. Several questions are yet to be answered. The first milestone will be to determine a processing sequence that yields repeatable crack free preforms and cataloguing their shrinkages, porosities and pore sizes which are currently believed to be the most critical property of the preforms.

After identifying the ideal processing conditions, the next hurdle would be to devise a way of embedding the pure silica core in the cladding preform. Currently proposed ideas include processing the sol-gel cladding around the fused core so that gel is formed around core. Other proposals involve making the cladding and then mechanically drilling a hole for the core to fill or forming the hole in the aerogels by removable a plastic tube.

Extra attention should also be focused on the mechanical approach of introducing holes into the preforms. It may be found to be a very viable means of manufacturing random holey fibers.

Once the above goals have been met, research efforts may now be focused on attenuation and improving the finer qualities of the random hole optical fibers for their specific uses.

References

[1] Knight, J. C., et al. “All-Silica Single-Mode Optical Fiber with Photonic Crystal Cladding.” Optics Letters, Volume 21, #19, (1996): 1547-1550

[2] Joannopoulos, J. D., Johnson S.G., “Photonic Crystals: Periodic Surprises in Electromagnetism” Materials Research Society Tutorial Series, MIT Chapter IAP, 2003

[3] Monro, T. M., et al. “Holey Fibers with Random Cladding Distributions.” Optics Letters, Volume 25, #4, (2000): 206-208

[4] Wang, S-H. “Sol-Gel Derived Silica Optics.” Dissertation. University of Florida, 1988

[5] Okazaki, H., et al. “Mechanical Strength Improvement of Sol-Gel Derived Dry Gels for Optical Fiber Preforms.” Journal of Non-Crystalline Solids, Volume 116, (1990): 87-92

[6] Ho K. M. et al, Photonic Band Gap Materials. 23-40. Ed. Soukoulis C. M. Kluwer Academic Publishers, 1995

[7] Joannapoulos, J. D., Meade, R. D., Winn, J. N. Photonic Crystals: Molding the flow of light. Princeton University Press, 1995

[8] Reynolds, A. L. Photonic Band Gap Materials Research, Opto-Electronics Research Group, University of Glasgow. 17 May, 2000 <www.elec.gla.ac.uk/groups/opto/photoniccrystal/Welcome.html >

[9] Ho, K. M. et al. Physical Review Letters, Volume 65, #24 (1990)

[10] Monro, T. M., et al. “Holey Fibers with Random Cladding Distributions.” Optics Letters, Volume 25, #4, (2000): 206-208

[11] Knight, J. C., et al. “All-Silica Single-Mode Optical Fiber with Photonic Crystal Cladding.” Optics Letters, Volume 21, #19, (1996): 1547-1550

[12] Pickrell, G., et al. “Novel Techniques for the Fabrication of Holey Optical Fibers”. Ed. Marcus, M. A., Culshaw B.: SPIE Fiber Optic Sensor Technology and Applications. Volume 4578. 2001 Newton, U.S.A.

[13] Birks, T. A., Knight, J. C., Russell, P. St. J. “Endlessly Single-Mode Photonic Crystal Fiber.” Optics Letters, Volume 22, #13(1997): 961-963

[14] Yoblanovich E., “Photonic Crystals: Semiconductors of Light.” Scientific American (December 2001): 47-55

[15] Ebelmen, J-J. Ann., 57 (1846)

[16] Brinker, C. J., Scherer, G.W. “Sol-Gel Science: The Physics and Chemistry of Sol-Gel Processing”, Academic Press 1990

[17] Pope, E. J. A., Mackenzie, J. D. “Sol-Gel Processing of Silica II. The Role of the Catalyst” Journal of Non-Crystalline Solids, Volume 87, (1986): 185-198
[18] James, P. F. “The Gel to Glass Transition: Chemical and Microstructural Evolution.” Journal of Non-Crystalline Solids, Volume 100, (1988): 93-114
[19] Jones, R. W. “Fundamental Principles of Sol-Gel Technology”, The Institute of Metals 1989
[20] Klein, L. C. “Sol-Gel Processing of Silicates.” Annual Review of Material Science, Volume 15, (1985): 227-248
[21] Haereid, S., et al. “Preparation and Properties of Monolithic Silica Xerogels from TEOS-Based Alcogels Aged in Silane Solutions.” Journal of Non-Crystalline Solids, Volume 186, (1995): 96-103
[22] Hench, L. L., West, J. K. “The Sol-Gel Process.” Chemical Review, Volume 90, (1989): 33-72
[23] Colby, M. W., Osaka, A., Mackenzie, J. D. “Temperature Dependence of the Gelation of Silicon Alkoxides.” Journal of Non-Crystalline Solids, Volume 99, (1988): 129-139
[24] Colby, M. W., Osaka, A., Mackenzie, J. D. “Effects of Temperature on Formation of Silica Gel.” Journal of Non-Crystalline Solids, Volume 82, (1986): 37-41
[25] Pajonk, G. M., et al. “Microstructural Characterization of Silica Aerogels Using Scanning Electron Microscopy.” Journal of Material Science, Volume 31, #21(1996): 5683-5689
[26] Brinker, C. J. “Sol-Gel Transition of Simple Silicates* 1.” Journal of Non-Crystalline Solids, Volume 48, (1982): 47-64
[27] S. Haereid et al. “Preparation and Properties of Monolithic Silica Xerogels from TEOS-Based Alcogels Aged in Silane Solutions.” Journal of Non-Crystalline Solids, Volume 186, (1995): 96-103
[28] Cerruti, M., et al. “Characterization of sol gel bioglasses with the use of simple model systems: a surface-chemistry approach.” Journal of Materials Chemistry, Volume 13, (2003): 1279-1286
[29] Alié C. et al. “Preparation of Low-Density Xerogels through Additives to TEOS-Based Alcogels.” Journal of Non-Crystalline Solids, Volume 246, (1999): 216-228
[30] Rao, A. V., et al. “Influence of Temperature on the Physical Properties of TEOS Silica Xerogels.” Ceramics International, Volume 25, (1999): 505-509
[31] Elias, E. A., “Pore Size Effects on the Thermal Stability of Sol-Gel Silica Monoliths” Thesis. University of Florida, 1989
[32] Einarsrud, M.-A. “Light Gels by Conventional Drying” Journal of Non-Crystalline Solids, Volume 225, (1998): 1-7

[33] Land, V. D., “Effect of Gel Modulus on the Porosity of Low-Density Silica” Journal of Non-Crystalline Solids, Volume 316, (2003): 238-245
[34] Sakka, S., Kamiya, K. “The Sol-Gel Transition in Hydrolysis of Metal Alkoxides in Relation to the Formation of Glass Fibers and Films” Journal of Non-Crystalline Solids, Volume 48, (1982): 31-46

Appendix A Detailed Account of Some of the Sol-Gel Recipes Implemented

Single-Step acid recipe by Brinker and Scherer [16] **

Materials	Percentage	Mole Ratios	Mols	Volume	
TEOS	6.700	1.000	0.1750	40.00	mL
Ethanol	25.800	3.851	0.6738	41.33	mL
HCl	0.200	0.030	0.0052	0.43	mL
H2O	67.300	10.045	1.7578	31.64	mL
R - ratio	10.045	14.92537313	Reaction Volume	113.40	mL

TEOS			WASHING SOLUTION		
Volume, V	40	mL	Volume, V	351.54	mL
Purity	98	% wt	Volume of Water, VH2O	70.31	mL
Density, dTEOS	0.93	g/mL	Volume of EtOH, VEtOH	281.23	mL
Mass, m	37.2	g			
Mass, mTEOS	36.456	g			
Molecular Mass, MTEOS	208.33	g/mol			
Moles of TEOS, nTEOS	0.1750	mol			

EtOH			AGING SOLUTION*		
Volume, V	41.33	mL	Volume, V	234.36	mL
Purity	100	% wt	Volume of TEOS, VTEOS	164.05	mL
Volume, VEtOH	41.33	mL	Volume of EtOH, VEtOH	70.31	mL
Density, dEtOH	0.75	g/mL	*for 2 of the 3 parts		
Mass, mEtOH	31.00	g			
Molecular Mass, MEtOH	46	g/mol			
Moles of EtOH, nEtOH	0.6738	mol			

HCl			1M HCl		
Volume, V	0.43	mL	Mdilute	1.0	mol/L
HCl Purity	37.25	% wt	Vdilute	50.00	mL
Volume, VHCl	0.16	mL	Mconc	12.1	mol/L
Density, d	1.19		Vconc	4.13	mL
molarity of	1	mol			

HCl		
Mass, mHCl	0.19	g
Molecular Mass, MHCl	36.46	g/mol
Moles of HCl, nHCl	0.0052	mol
H2O		
Volume, V	31.64	mL
Purity	100	% wt
Volume, VH2O	31.64	mL
Density, dH2O	1	g/mL
Mass, mH2O	31.64	g
Molecular Mass, MH2O	18	g/mol
Moles of H2O, nH2O	1.7578	mol

Single-Step base recipe by Brinker and Scherer [16] **

Materials	Percentage	Mols	Volume (mL)
TEOS	6.7	0.1750	40.00
Ethanol	25.8	0.6738	41.33
NH3*	0.2	0.0052	2.54
H2O	67.3	1.7578	31.64
R - ratio	10	Total Volume	115.51

*of 1M NH4OH

TEOS			H2O		
Volume, V	40	mL	Volume, V	31.64	mL
Purity	98	%	Purity	100	%
Volume, VTEOS	39.2	mL	Volume, VH2O	31.64	mL
Density, dTEOS	0.93	g/mL	Density, dH2O	1	g/mL
Mass, mTEOS	36.456	g	Mass, mH2O	31.64	g
Molecular Mass, MTEOS	208.33	g/mol	Molecular Mass, MH2O	18	g/mol
Moles of TEOS, nTEOS	0.1750	mol	Moles of H2O, nH2O	1.7578	mol

EtOH			WASHING SOLUTION		
Volume, V	41.33	mL			
Purity	100	%	Volume, V	358.07	mL
Volume, VEtOH	41.33	mL	Volume of Water, VH2O	71.61	mL
Density, dEtOH	0.75	g/mL	Volume of EtOH, VEtOH	286.45	mL
Mass, mEtOH	31.00	g			
Molecular Mass, MEtOH	46	g/mol	AGING SOLUTION*		
Moles of EtOH, nEtOH	0.6738	mol	Volume, V	238.71	mL
			Volume of TEOS, VTEOS	167.10	mL
NH4OH			Volume of EtOH, VEtOH	71.61	mL
Volume, V	2.54	mL	*for 2 of the 3 parts		
NH3 Purity*	48.57	%			
Volume, VNH4OH	2.54	mL			
Molarity of NH4OH	1	mol/L	1M NH4OH		
Mass, mNH4OH	0.183	g	Mdilute	1.0	mol/L
Molecular Mass,	35.03	g/mol	Vdilute	50.00	mL

MNH4OH					
Moles of NH3, nNH3	0.0052	mol	Mconc	14.8	mol/L
Moles of NH4OH, nNH4OH	0.0025	mol	Vconc	3.38	mL

*17g NH3 per 1L NH4OH

Modified Single-Step base recipe from Berkeley Labs at Berkeley by way of Ashley White

Materials	Purity/%	Molarity/M	Volume/mL	Moles	Mol %
TEOS	98		12	0.0525	2.74
Ethanol	100		12	0.1957	10.21
diH2O	100		30	1.6667	86.98
NH4OH	30**		0.06	0.0009	0.05
NH4F	-	0.5	0.72	0.00036	0.02
R - ratio	32	Ttl. Vol.	54.78	1.9161	100

TEOS			EtOH		
Volume, V	12	mL	Volume, V	12	mL
Purity	98	% wt	Purity	100	% wt
Density, dTEOS	0.93	g/mL	Volume, VEtOH	12	mL
Mass, m	11.16	g	Density, dEtOH	0.75	g/mL
Mass, mTEOS	10.9368	g	Mass, mEtOH	9	g
Molecular Mass, MTEOS	208.33	g/mol	Molecular Mass, MEtOH	46	g/mol
Moles of TEOS, nTEOS	0.0525	mol	Moles of EtOH, nEtOH	0.1957	mol

0.5M NH4F			diH2O		
Molarity of NH4F	0.5	mol/L	Volume, V	30	mL
Mass, mNH4F	18.52	g	Purity	100	% wt
NH4F Purity	98	% wt	Volume, VH2O	30	mL
Mass, m	18.898	g	Density, dH2O	1	g/mL
Moles of NH4F, nNH4F	0.5	mol	Mass, mH2O	30	g
Molecular Mass, MNH4F	37.04	g/mol	Molecular Mass, MH2O	18	g/mol
Volume, VNH4F	1000	mL	Moles of H2O, nH2O	1.6667	mol

100mL 0.5M NH4F		
Volume, VH2O	100	mL
Mass, m	1.852	g

NH4OH		
Purity**	29.3	% wt
Molecular Mass, MNH4OH	35.03	g/mol
Density, DNH4OH	0.9	g/mL
Molarity of NH4OH	14.8	mol/L

**Recipe required 0.06mL 30%wt NH4OH

Single-Step acid recipe by Einarsrud [32]

Material (I/II)*	Percentage	Mole Ratio	Mols	Volume	
TEOS - I	11.896	1	0.2187	50.00	mL
Ethanol - I	46.393	3.9	0.8531	52.32	mL
NH4OH - II	0.068	0.0057	0.0012	0.17	mL
HCl - I	0.009	0.00078	0.0002	0.01	mL
H2O - I & II	41.635	3.5	0.7656	13.78	mL
R - ratio	4	8.40648	Reaction Volume	116.29	mL

*Step in which material is used

TEOS			H2O		
Volume, V	50	mL	Volume, V	13.78	mL
Purity	98	% wt	Purity	100	% wt
Density, dTEOS	0.93	g/mL	Volume, VH2O	13.78	mL
Mass, m	46.5	g	Density, dH2O	1	g/mL
Mass, mTEOS	45.57	g	Mass, mH2O	13.781	g
Molecular Mass, MTEOS	208.33	g/mol	Molecular Mass, MH2O	18	g/mol
Moles of TEOS, nTEOS	0.2187	mol	Moles of H2O, nH2O	0.7656	mol

EtOH			WASHING SOLUTION		
Volume, V	52.32	mL	Volume, V	360.50	mL
Purity	100	% wt	Volume of Water, VH2O	72.10	mL
Volume, VEtOH	52.32	mL	Volume of EtOH, VEtOH	288.40	mL
Density, dEtOH	0.75	g/mL		360.50	
Mass, mEtOH	39.242	g	AGING SOLUTION		
Molecular Mass, MEtOH	46	g/mol	Volume, V	360.50	mL
Moles of EtOH, nEtOH	0.8531	mol	Volume of TEOS, VTEOS	252.35	mL
			Volume of EtOH, VEtOH	108.15	mL

NH4OH					
Volume, V	0.17	mL	1M NH4OH		
Purity	28	% wt	Mdilute	1.0	mol/L
Volume, VNH4OH	0.17	mL	Vdilute	50.00	mL
Density, DNH4OH	0.9	g/mL	Mconc	14.8	mol/L
Mass, m	0.156	g	Vconc	3.38	mL
molarity of NH4OH	1	mol/L			
Mass, mNH4OH	0.044	g			

Molecular Mass, MNH4OH	35.03	g/mol
Moles of NH4OH, nNH4OH	0.0012	mol
HCl		
Volume, V	0.014	mL
HCl Purity	37.25	% wt
Volume, VHCl	0.00523	mL
Density, d	1.19	
molarity of HCl	1	mol
Mass, mHCl	0.0062	g
Molecular Mass, MHCl	36.46	g/mol
Moles of HCl, nHCl	0.00017	mol

1M HCl		
Mdilute	1.0	mol/L
Vdilute	50.00	mL
Mconc	12.1	mol/L
Vconc	4.13	mL

2-Step acid-base recipe by Haereid [21]

Material	Percentage	Mol Ratio	Mols	Volume	
TEOS	11.8956	1	0.2187	50.00	mL
Ethanol	46.3928	3.9	0.8531	52.32	mL
NH4OH	0.0678	0.0057	0.0012	0.17	mL
HCl	0.0093	0.00078	0.0002	52.32	mL
H2O	41.6345	3.5	0.7656	13.78	mL
R - ratio	3.5	8.40648	Reaction Volume	168.60	mL

TEOS					
Volume, V	50	mL	H2O		
Purity	98	% wt	Volume, V	13.781	mL
Density, dTEOS	0.93	g/mL	Purity	100	% wt
Mass, m	46.5	g	Volume, VH2O	13.781	mL
Mass, mTEOS	45.57	g	Density, dH2O	1	g/mL
Molecular Mass, MTEOS	208.33	g/mol	Mass, mH2O	13.781	g
Moles of TEOS, nTEOS	0.2187	mol	Molecular Mass, MH2O	18	g/mol
			Moles of H2O, nH2O	0.7656	mol

EtOH		
Volume, V	52.32	mL
Purity	100	% wt
Volume, VEtOH	52.32	mL
Density, dEtOH	0.75	g/mL
Mass, mEtOH	39.242	g
Molecular Mass, MEtOH	46	g/mol
Moles of EtOH, nEtOH	0.8531	mol

NH4OH			1M NH4OH		
Volume, V	0.17	mL	Mdilute	1.0	mol/L
Purity	28	% wt	Vdilute	50.00	mL
Volume, VNH4OH	0.17	mL	Mconc	14.8	mol/L
Density, DNH4OH	0.9	g/mL	Vconc	3.38	mL
Mass, m	0.156	g			
Molarity of NH4OH	1	mol/L			
Mass, mNH4OH	0.044	g			
Molecular Mass, MNH4OH	35.03	g/mol			
Moles of NH4OH,	0.00125	mol			

nNH4OH		

HCl			1M HCl		
Volume, V	0.014	mL	Mdilute	1.0	mol/L
HCl Purity	37.25	% wt	Vdilute	50.00	mL
Volume, VHCl	0.00523	mL	Mconc	12.1	mol/L
Density, d	1.19		Vconc	4.13	mL
molarity of HCl	1	mol			
Mass, mHCl	0.00622	g			
Molecular Mass, MHCl	36.46	g/mol			
Moles of HCl, nHCl	0.00017	mol			

Single-Step acid recipe by Land [33]

Material - STEP I			
	Purity/%	Molarity/M	Volume/mL
TEOS	98		244
Ethanol	100		244
HCl	-	1	0.8
H2O	100		19.6
R - ratio	1		
		Total Volume	508.4

Material - STEP II*			
	Purity/%	Moles	Volume/mL
Acidic Sol			50
TEOS Present		0.104981192	
TMMOS**	0.99	0.057739656	7.96
NH4OH - II		0.00025	5

*calculated for each 50mL sample!!!!! 62.96

**0.55 mol/mol Silicone

So for 8 samples	
	Volume/mL
Acidic Sol	400
TEOS Present	191.97
TMMOS	63.68
NH4OH - II	40
Total Volume	695.6595245

TEOS			TMMOS		
Volume, V	244	mL	Volume, V	63.68	mL
Purity	98	% wt	Purity	99	% wt
Density, dTEOS	0.93	g/mL	Density, dTMMOS	0.756	g/mL
Mass, m	226.92	g	Mass, m	48.146	g
Mass, mTEOS	222.382	g	Mass, mTMMOS	47.664	g
Molecular Mass, MTEOS	208.33	g/mol	Molecular Mass, MTMMOS	104.23	g/mol
Moles of TEOS, nTEOS	1.0674	mol	Moles of TMMOS, nTMMOS	0.4573	mol

EtOH			diH2O		
Volume, V	244	mL	Volume, V	19.6	mL
Purity	100	% wt	Purity	100	% wt
Volume, VEtOH	244	mL	Volume, VH2O	19.6	mL

Density, dEtOH	0.75	g/mL	Density, dH2O	1	g/mL
Mass, mEtOH	183	g	Mass, mH2O	19.6	g
Molecular Mass, MEtOH	46	g/mol	Molecular Mass, MH2O	18	g/mol
Moles of EtOH, nEtOH	3.9783	mol	Moles of H2O, nH2O	1.0889	mol

NH4OH					
Volume, V	0.035	mL	1M NH4OH		
Purity	28	% wt	Mdilute	1.0	mol/L
Volume, VNH4OH	0.035	mL	Vdilute	50.00	mL
Density, DNH4OH	0.9	g/mL	Mconc	14.8	mol/L
Mass, m	0.031	g	Vconc	3.38	mL
molarity of NH4OH	1.0	mol/L	0.05M NH4OH		
Mass, mNH4OH	0.0088	g	Mdilute	0.05	mol/L
Molecular Mass, MNH4OH	35.03	g/mol	Vdilute	50.00	mL
Moles of NH4OH, nNH4OH	0.00025	mol	Mconc	1	mol/L
			Vconc	2.50	mL

HCl					
Volume, V	0.8	mL			
HCl Purity	37.25	% wt	1M HCl		
Volume, VHCl	32.71	mL	Mdilute	1.0	mol/L
Density, d	1.19		Vdilute	50.00	mL
molarity of HCl	1	mol	Mconc	12.1	mol/L
Mass, mHCl	38.919	g	Vconc	4.13	mL
Molecular Mass, MHCl	36.46	g/mol			
Moles of HCl, nHCl	1.0674	mol			

Single-Step acid recipe by Sakka and Kamiya [34]

Materials	Mass (g)	Moles	Mole Percentage	Volume	
TEOS	84.75	0.4068	4.544	92.99	mL
Ethanol	18.75	0.4076	4.553	25.00	mL
HCl/TEOS RATIO ***	0.01	0.0041	0.045	0.12	mL
H2O	146.4	8.1333	90.857	146.40	mL
R - ratio	19.99	8.9518	Reaction Volume	264.51	mL

TEOS			EtOH		
Volume, V	92.99	mL	Volume, V	25	mL
Purity	98	% wt	Purity	100	% wt
Density, dTEOS	0.93	g/mL	Volume, VEtOH	25	mL
Mass, m	86.480	g	Density, dEtOH	0.75	g/mL
Mass, mTEOS	84.75	g	Mass, mEtOH	18.75	g
Molecular Mass, MTEOS	208.33	g/mol	Molecular Mass, MEtOH	46	g/mol
Moles of TEOS, nTEOS	0.4068	mol	Moles of EtOH, nEtOH	0.4076	mol

HCl			H2O		
Volume, V	0.125	mL	Volume, V	146.40	mL
HCl Purity	100	% wt	Purity	100	% wt
Volume, VHCl	0.125	mL	Volume, VH2O	146.4	mL
Density, d	1.19	g/mL	Density, dH2O	1	g/mL
molarity of HCl	1	mol	Mass, mH2O	146.4	g
Mass, mHCl	0.148	g	Molecular Mass, MH2O	18	g/mol
Molecular Mass, MHCl	36.46	g/mol	Moles of H2O, nH2O	8.1333	mol
Moles of HCl, nHCl	0.0041	mol			

1M HCl		
Mdilute	1.0	mol/L
Vdilute	50.00	mL
Mconc	12.1	mol/L
Vconc	4.13	mL

Single-Step acid recipe by Wang [4]

Materials	Percentage	Moles	Volume	
TEOS	17.26	0.8006	183	mL
Ethanol	64.33	2.9837	183	mL
Oxalic Acid($C_2H_2O_4$)	1.14	0.0529	N/A	mL
H2O	17.26	0.8006	14.41	mL
	100.00	4.6378	380.41	mL

R = H2O/TEOS	1
DCCA = Oxalic/TEOS	0.0661

TEOS			C2H2O4		
Volume, V	183	mL	Volume, V	N/A	mL
Purity	98	%	Purity	98	%
Volume, VTEOS	179.34	mL	Volume, $VC_2H_2O_4$	N/A	mL
Density, dTEOS	0.93	g/mL	Density, $dC_2H_2O_4$	N/A	g/mL
Mass, mTEOS	166.786	g	Mass, mHCl	4.764	g
Molecular Mass, MTEOS	208.33	g/mol	Molecular Mass, $MC_2H_2O_4$	90.03	g/mol
Moles of TMOS, nTEOS	0.8006	mol	Moles of HCl, $nC_2H_2O_4$	0.0529	mol

EtOH			H2O		
Volume, V	183	mL	Volume, V	14.41	mL
Purity	100	%	Purity	100	%
Volume, VEtOH	183	mL	Volume, VH_2O	14.41	mL
Density, dEtOH	0.75	g/mL	Density, dH_2O	1	g/mL
Mass, mEtOH	137.25	g	Mass, mH_2O	14.41	g
Molecular Mass, MEtOH	46	g/mol	Molecular Mass, MH_2O	18	g/mol
Moles of EtOH, nEtOH	2.9837	mol	Moles of H_2O, nH_2O	0.8006	mol

2-Step acid-base (B2) recipe by from Sandia National Labs by way of Scott T. Reed

	Purity/%	Molarity/M	Volume/mL	Moles
TEOS	98		61	0.2669
Ethanol	100		61	0.9946
HCl		1	0.2	0.0002
H2O	100		4.8	0.2667
NH4OH - II*		0.25	12.7	0.0032
R - ratio	1			1.5315
	Volume of Acidic sol, less NH3		127	

Materials - STEP II			
	Molarity/M	Moles	Vol/mL
Acidic Sol			127
NH4OH - II	0.25	0.003175	12.7

TEOS			EtOH		
Volume, V	61	mL	Volume, V	61	mL
Purity	98	% wt	Purity	100	% wt
Density, dTEOS	0.93	g/mL	Volume, VEtOH	61	mL
Mass, m	56.73	g	Density, dEtOH	0.75	g/mL
Mass, mTEOS	55.595	g	Mass, mEtOH	45.75	g
Molecular Mass, MTEOS	208.33	g/mol	Molecular Mass, MEtOH	46	g/mol
Moles of TEOS, nTEOS	0.2669	mol	Moles of EtOH, nEtOH	0.9946	mol

NH4OH			0.25M NH4OH		
Volume, V	0.44	mL	Mdilute	0.25	mol/L
Purity	28	% wt	Vdilute	50.00	mL
Volume, VNH4OH	0.44	mL	Mconc	14.8	mol/L
Density, DNH4OH	0.9	g/mL	Vconc	0.84	mL
Mass, m	0.397	g			
Molarity of NH4OH	0.25	mol/L	1M HCl		
Mass, mNH4OH	0.1112	g	Mdilute	1.0	mol/L
Molecular Mass, MNH4OH	35.03	g/mol	Vdilute	50.00	mL
Moles of NH4OH, nNH4OH	0.00318	mol	Mconc	12.1	mol/L
			Vconc	4.13	mL

HCl					
Volume, V	0.2	mL	diH2O		
HCl Purity	37.25	% wt	Volume, V	4.8	mL
Volume, VHCl	0.006	mL	Purity	100	% wt
Density, d	1.19		Volume, VH2O	4.8	mL

Molarity of HCl	1	mol	Density, dH2O	1	g/mL
Mass, mHCl	0.0073	g	Mass, mH2O	4.8	g
Molecular Mass, MHCl	36.46	g/mol	Molecular Mass, MH2O	18	g/mol
Moles of HCl, nHCl	0.0002	mol	Moles of H2O, nH2O	0.2667	mol

Appendix B Design of Experiments

The temperature and the amounts of catalyst and buffer were selected as the design characteristics of the experiment.

		Factor Levels		
Factors	Temperature (^{o}C)	25	40	60
	Amount of Catalyst (mL)	0.06	0.12	0.18
	Amount of Buffer (mL)	0.24	0.48	0.72

Catalyst 30% NH_4OH
Buffer 0.5M NH_4F

Experimental Setup
The L-9 array was selected as the best design for testing three factors at three levels

Trial	Temperature, T	Amount of Buffer, B	Amount of Catalyst, C
1	25	0.24	0.06
2	25	0.48	0.12
3	25	0.72	0.18
4	40	0.24	0.12
5	40	0.48	0.18
6	40	0.72	0.06
7	60	0.24	0.18
8	60	0.48	0.06
9	60	0.72	0.12

Results

Trial	Results (MMM")
1	>720"
2	>720"
3	>720"
4	>120"
5	>120"
6	>040"
7	>120"
8	>038"
9	>022"

Results are measured in hours and minutes as the time taken to gel. For trials 1, 2 and 3, no data was taken beyond 12 hours, and for 4, 5 and 7 no data was taken beyond 2 hours.

Vita

Frederick Paa Kwesi Ellis was born and raised by Dr. Samuel Ellis and Christiana Ellis in the West African Republic of Ghana. After completing kindergarten at the First Baptist Nursery School, he continued his Primary (Elementary) School Studies at the Tema Parents' Association School. While undergoing secondary (US Junior High and High School equivalent) education at Mfantsipim School, he compiled Ordinary Level and Advanced Level Certificates from the West African Examinations Council before heading out to the United States of America for college.

His first two years of college was at Delaware State University where he studied chemistry and biology before transferring to Virginia Tech in the fall of 1998. While at Delaware, he worked as a Peer Tutor in math and sciences and in the summer of 1998 he embarked upon his first research assignment under the direction of Dr. Ronald Wilkinson of the Chemistry Department at Delaware State University. In the fall semester of 2000, he graduated with a Bachelor of Science in Chemical Engineering from Virginia Tech. In the fall semester of 2001, Fred was a part-time graduate student and worked as a Research Assistant to Dr. Gau-Quan Lu. Under the supervision of Dr. Lu's doctorate candidate, Fred worked on a project focused on fabricating and evaluating the effectiveness of solder-bonded devices on substrates versus the more established wire-bonded devices.

In the fall of 2002, as a full-time graduate student, Fred was awarded a graduate research assistantship from the Center for Photonics Technology from whence he commenced on his current project for this masters thesis. Upon graduation Fred Ellis will be working as a Process Engineer for Micron Technology, Inc.